การศึกษาและพัฒนากระบวนการผลิตสารเคลือบผิวพอลิเมอร์สำหรับเซลล์แสงอาทิตย์

ผศ.ดร. สุรัตน์ อารีรัตน์
กัณฑมาศ ถาวร

A THESIS SUBMITTED IN PARTIAL FULFILLMENT

OF THE REQUIREMENT FOR THE DEGREE OF

MASTER OF ENGINEERING IN CHEMICAL ENGINEERING

SCHOOL OF GRADUATE STUDIES

KING MONGKUT'S INSTITUTE OF TECHNOLOGY LADKRABANG

2007

KMITL-2007-EN-M-220-026

Thesis Certification

School of Graduate Studies

King Mongkut's Institute of Technology Ladkrabang

Thesis Title	Study and Development of Film processing of Polymer Based Encapsulant for Photovoltaic Modules
Student	Miss Kanthamas Thaworn
Student ID.	48060118
Degree	Master of Engineering
Program	Chemical Engineering
Thesis Advisor	Assist.Prof.Dr.Surat Areerat

EXAMINERS		SIGNATURES
Assoc.Prof.Dr.Prakob	Kitchaiya	
Asst.Prof.Dr.Apinan	Namkanisorn	
Dr.Sutasinee	Neramittagapong	
Dr.Wuttipong	Rungseesantivanon	
Asst.Prof.Dr.Surat	Areerat	

Date 23 July 2007 **Time** 11.30-13.30 pm.

Place room E12-404 Faculty of Engineering

(Assoc.Prof.Dr.Jarruwat Charoensuk)
Dean

Date...28.....**Month**...September.....**Year**...2007....

หัวข้อวิทยานิพนธ์	การศึกษาและพัฒนากระบวนการผลิตสารเคลือบผิวพอลิเมอร์สำหรับเซลล์แสงอาทิตย์
นักศึกษา	นางสาวกัณฑมาศ ถาวร
รหัสประจำตัว	48060118
ปริญญา	วิศวกรรมศาสตรมหาบัณฑิต
สาขาวิชา	วิศวกรรมเคมี
พ.ศ.	2550
อาจารย์ที่ปรึกษาวิทยานิพนธ์	ผศ.ดร. สุรัตน์ อารีรัตน์

บทคัดย่อ

งานวิจัยนี้ทำการศึกษาและพัฒนาเอธิลีนไวนิลอะซิเตตสำหรับหุ้มเซลล์แสงอาทิตย์ จากการศึกษา พบว่าปฏิกิริยาการเชื่อมโยงซึ่งระหว่างเอธิลีนไวนิลอะซิเตตและสารอินทรีย์เปอร์ออกไซด์ร่วมกับสารคู่ควบ เป็นปรากฏการณ์ที่สำคัญที่เกิดขึ้นระหว่างกระบวนการเคลือบผิวเซลล์แสงอาทิตย์ ปัจจัยสำคัญสำหรับปฏิกิริยาดังกล่าวคือสารอินทรีย์เปอร์ออกไซด์ ดังนั้นในงานวิจัยนี้จึงได้ทำการศึกษาผลของสารอินทรีย์เปอร์ออกไซด์ 3 ชนิด ได้แก่ สารไดอัลคิวเปอร์ออกไซด์ สารเพอร์รอกซีเอส์เทอร์เปอร์ออกไซด์ และสารเพอร์รอกซีคีตอลเปอร์ออกไซด์ พบว่า สารไดอัลคิวเปอร์ออกไซด์ ไม่เหมาะสำหรับนำมาใช้ในการผลิตสารห่อหุ้มเซลล์แสงอาทิตย์ เนื่องจากมีค่าอุณหภูมิครึ่งชีวิตสูงและเกิดผลิตภัณฑ์ที่ทำให้เกิดการเปลี่ยนสีของสารห่อหุ้ม สำหรับสารเพอร์รอกซีเอส์เทอร์เปอร์ออกไซด์ซึ่งเป็นสารเปอร์ออกไซด์ทางการค้าสำหรับการผลิตสารห่อหุ้มเซลล์แสงอาทิตย์นั้น สามารถเกิดการสุกตัวได้ที่ในช่วงอุณหภูมิ 150 ถึง 160 องศาเซลเซียส โดยสามารถเกิดการสุกตัวอย่างสมบูรณ์ได้ภายในเวลา 5 ถึง 8 นาที และสำหรับสารเพอร์รอกซีคีตอลเปอร์ออกไซด์ พบว่ามีประสิทธิภาพสูงสุด เนื่องจากสามารถเกิดการสุกตัวอย่างสมบูรณ์ได้ภายในเวลา 3 นาที

จากการศึกษาพบว่า เม็ดพลาสติกเอธิลีนไวนิลอะซิเตตซึ่งผลิตได้ในประเทศนั้น มีความสามารถที่จะนำไปใช้งานทดแทนเม็ดพลาสติกจากการนำเข้าได้ นอกจากนี้ สูตรการผลิตโดยใช้เม็ดพลาสติกเอธิลีนไวนิลอะซิเตตซึ่งผลิตได้ในประเทศ ร่วมกับสารเพอร์รอกซีคีตอลเปอร์ออกไซด์ปริมาณ 0.1 ส่วนต่อร้อยส่วนของเม็ดพลาสติก โดยน้ำหนัก เป็นสูตรการผลิตที่มีคุณสมบัติในการเป็นสารห่อหุ้มได้ดี นอกจากนี้ได้ทำการศึกษาการเกิดปฏิกิริยาการเชื่อมโยงที่ด้วยเครื่องมือ Moving Die Rheometer (MDR) ซึ่งสามารถศึกษาปฏิกิริยาที่เกิดขึ้นภายใต้สภาวะอุณหภูมิคงที่ และจากการประยุกต์ใช้วิธี Isoconversional model-free method ในการศึกษาจลนศาสตร์ของปฏิกิริยาพบว่าสามารถประมาณค่าพลังงานกระตุ้นของปฏิกิริยาการเชื่อมโยงของเอธิลีนไวนิลอะซิเตตกับ

สารไดอัลคิวเปอร์ออกไซด์ และสารเพอร์รอกซีเอส์เทอร์เปอร์ออกไซด์ ได้ 96 และ 75 กิโลจูลต่อโมล ตามลำดับ ซึ่งสอดคล้องกับการคำนวณด้วยคอมพิวเตอร์ด้วยวิธี Model-fitting method โดยสมมติให้ ปฏิกิริยาที่เกิดขึ้นเป็นปฏิกิริยาอันดับหนึ่ง แต่วิธีการนี้ไม่เหมาะสมสำหรับปฏิกิริยาที่มีความซับซ้อนมากดังเช่นปฏิกิริยาการเชื่อมโยงของเอธิลีนไวนิลอะซิเตตและสารเพอร์รอกซีเอส์เทอร์เปอร์ออกไซด์ นอกจากนี้ยังสามารถประยุกต์ใช้เครื่องมือ MDR ในการประมาณปริมาณเจล ซึ่งสัมพันธ์กับองศาของพันธะเชื่อมโยงแบบร่างแห (degree of crosslinking) โดยอาศัยความสัมพันธ์ของอัตราส่วนแรงบิด ซึ่งเป็นฟังก์ชันของ ปริมาณแอกทีฟออกซิเจนของสารอินทรีย์เปอร์ออกไซด์ และค่าดรรชนีการไหลของเม็ดพลาสติกเอธิลีนไวนิลอะซิเตต ซึ่งการประมาณค่าด้วยวิธีนี้สามารถให้ค่าปริมาณเจลได้ใกล้เคียงกับการหาค่าด้วยวิธีการวัดปริมาณเจลแบบดังเดิม

Thesis Title	Study and Development of Film processing of Polymer Based Encapsulant for Photovoltaic Modules
Student	Miss Kanthamas Thaworn
Student ID.	48060118
Degree	Master of Engineering
Program	Chemical Engineering
Year	2007
Thesis Advisor	Asst.Prof.Dr. Surat Areerat

ABSTRACT

This research aims to investigate the knowledge of encapsulation materials for solar cells and to develop EVA-based encapsulant using domestic raw materials for the purpose of cost reduction. EVAs which contain 18, 28 and 33 %wt VA contents were determined. The crosslinking reactions with organic peroxides and silane coupling agent are essential phenomena during the lamination-curing process. The important key factor of crosslinking reactions of EVA-based encapsulant during lamination-curing process is organic peroxide. Three classes of organic peroxide candidates which are dialkyl peroxide, peroxyester peroxide and peroxyketal peroxide were studied. Dialkyl peroxide is not suitable because it has high half-life temperature and its by-products can discolor the final product. Peroxyester peroxide as a commercial is good for curing at temperature in range of 150 to 160°C which accomplished ultimate cure within 5 to 8 minutes. As well as the peroxyketal peroxide has higher performance which decreased optimum cure time to 3 minutes. The domestic EVA resin, which contains 28 %wt VA conient (EVA-28), is able to optimize cure as the commercial EVA 33 %wt VA content (EVA-33). Furthermore, the EVA-28 compounded with 0.10 phr of peroxyketal peroxide has considerably good performance for the encapsulant formulation. Thus, it would be possible to use the domestic EVA for solar cell encapsulant.

In addition, this research applied the MDR to determine crosslinking behavior. This apparatus is suitable for real-time isothermal crosslinking reaction study. The isoconversional model-free method was applied to estimate the activation energy of EVAs/Peroxide crosslinking reactions. The crosslinking reactions of EVA-33/Dialkyl peroxide and EVA-33/Peroxyester peroxide can be estimated approximately 96 and 75 kJ/mol which are similar to the first-order

reaction by model-fitting method using computer programmed calculation. On the other hand, it is not sufficient for estimation of the activation energy for manifold reactions likewise the crosslinking reactions of EVA-33/Peroxyketal peroxide. Moreover, the MDR measurement can be used to estimate the gel content by using the correlation of torque ratio $(\tau-\tau_0)/\tau_0$ which achieved the difference less than 3% from the conventional gel method.

ACKNOWLEDGEMENTS

This thesis could not be completed without the assistance of many persons to whom I would like to express my appreciation.

First, I would like to thank my advisor, Asst.Prof.Dr. Surat Areerat, who has given me many helpful suggestions, useful advice and fruitful discussions during the undertaken research.

I would like to thank Mr. Watchara Lekhapanyaporn from Arkema Pte. Ltd. and Ms.Piyathip Ussavarungsi from JJ-Degussa Chemicals (Thailand) Ltd. for providing chemicals and information which led to more detailed investigation in this work. Moreover, I would like to acknowledge Bangkok Solar Co.,Ltd. for commercial encapsulant sample as well as technical visiting and useful information for improvement this research approach. I would like to show gratitude to the Polymer Science Program, Faculty of Science, Prince of Songkha University for providing the MDR instrument as well as there staff's helpfulness and kindness.

I am grateful to the National Research Council of Thailand which provided financial support for this research.

Special thanks go to my friends at KMITL for helping me at any time.

Finally, I am very grateful to my family for all love, caring, understanding and motivation throughout my life.

Kanthamas Thaworn

Contents

Contents (cont.)

Contents (cont.)

List of Tables

List of Figures

List of Figures (cont.)

Figures Page

List of Figures (cont.)

Figures Page

Chapter 1

Introduction

1.1 Background

Energy is a factor of the well being of people and is an essential driving force for commercial and industrial potentials of countries. The global energy consumption is considerably increasing. Fossil fuel is the main source for our energy supplies. Unfortunately, fossil fuel is an unsustainable resource and caused a lot of pollution as well as climate changes.

Therefore, renewable energy is essentially required to support the demand of energy consumption. Solar energy is a sustainable energy source which can be converted directly into electricity using photovoltaic (PV) modules. The term "photovoltaic" is derived by combining the Greek word for light, *photos*, with *volt*, the name of the unit of electromotive force (i.e. an electric current). The discovery of the photovoltaic effect in 1839 is generally credited to the French physicist Edmond Becquerel. In 1953, the Chapin-Fuller-Pearson team, building on earlier Bell labs research on the PV effect in silicon, produced 'doped' silicon sliced that were much more efficient than earlier devices in producing electricity from light. In 1958, however, solar cells were used to power a small radio transmitter in the second US space satellite, Vanguard I. Following this first successful demonstration, the use of PV as a power source for spacecraft has become almost universal. Rapidly progress in increasing the efficiency and reducing the cost of PV cells has been made over the past few decades [1]. Their terrestrial uses are now widespread. PV modules provide an independent, reliable electrical power source at the point of use, making it particularly suited to remote locations. Today, PV systems have an important use in areas remote from an electrical grid. They provide power for water pumping, lighting, vaccine refrigeration, telecommunications and many other applications. European Commission [2] reported that in 2005, the PV industry continued its impressive growth and delivered worldwide some 1,700 mega peak watts (MWp) of PV generators. In the past 5 years, the average annual world growth rate was above 40%, making the further increase of production. An investment report published in 2004 by Credit Lyonnais Security Asia forecasted that the PV sector had a realistic potential to expand from $ 7 billion in 2004 to $ 30 billion in 2010.

1.1.1 PV module components

PV systems are essentially divided into two major parts: the PV modules and the balance of system. The PV module includes solar cells, electrical connections and packing as shown in Figure 1.1; Table 1.1 describes the PV module components. The balance of system includes components for managing the power provided by the cells, either storing it for later use in a battery system, or adapting the power to a form that can be interfaced with the existing electric grid, or often both [3].

There are currently two major types of solar modules: conventional (e.g. monocrystalline, polycrystalline silicon and gallium arsenide (GaAs) compound semiconductor) and thin-film (i.e. amorphous silicon).

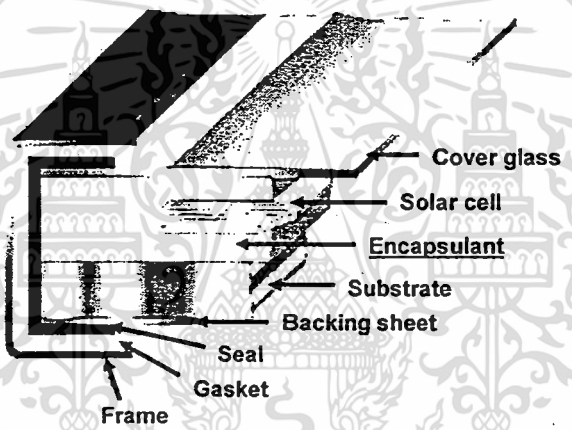

Figure 1.1 Schematic of flat plate PV module components [3].

Table 1.1 Description of PV module components [3]

Subcomponent	Description
Solar Cell	A PV cell is any device that transforms light energy directly onto electric energy. Current cells consist primarily of a semiconductor material, in which photons are absorbed from the incoming light to create free electron.
Top Surface	The top surface, usually glass or transparent plastic, allows light to enter the cell, while protecting the delicate cells from damages. It often has an anti-reflection coating as well, to increase the fraction of light transmitted.
Encapsulant	An encapsulant is used to provide adhesion between the solar cell, the top surface and the rear layer. It should be stable at elevated temperatures and high UV exposure as well as optically transparent and low thermal resistance.

Table 1.1 (cont.)

Subcomponent	Description
Rear Layer	The rear layer protects the back surface of the module, and prevents water and gases from entering the module.
Electrical Connection	Metal conductors carry electrons out of the cells, connecting the cells in the module in series or parallel, and carry electricity out of the module.
Frame	The frame adds structure to the module, and can attach to the mounting structure.

Sterzinger and Svrcek [3] estimated the components cost of PV module which includes 67.5% of solar cells, 8.9% of electrical connection and 23.6% of module packing which consists of the top surface, encapsulant, rear layer and frame.

1.1.2 PV encapsulant

The encapsulant is necessary for electrical isolation, mechanical protection of the solar cells, and corrosion protection of the metal contacts and interconnection system for more than 20 years of outdoor exposure in even the most severe terrestrial climate [4]. It must have a high transmission in the wavelengths which can used by the solar cells in the PV module. For silicon solar cells the top surface and encapsulant must have high transmission of light in the wavelength range of 0.35 to 1.1 μm. The specifications of encapsulant material are represented in Table 1.2. Nowadays low cost solar cells are developed then the encapsulation materials will become a dominant cost in a finished PV modules especially in the thin film PV manufacturing.

Ethylene vinyl acetate (EVA) copolymer is the most commonly used for PV modules encapsulant because of it is high cohesive strength, excellent adhesion to a wide range of substrates, high transparency, weatherability, and can be processed by dry-film lamination method. EVA comes in thin sheets which are inserted between the solar cells, the top surface and the rear layer. This sandwich is then heated to 150°C to crosslink the EVA and bond the module together.

A major source of EVA resin is Elvax 150™, manufactured by DuPont. Two widely used EVA films are designated by Springborn Laboratories as A9918P and 15295P grades [5].

Table 1.2 Encapsulant material specifications [4-5]

1. Total hemisphere light transmission through a 20 mils thick film integrated over the wavelength range from 400-1,100 nm	> 90% of incident
2. Gel content of crosslink film	80-90%
3. Glass transition temperature	< -40°C
4. Hydrolysis, Hazing or clouding	None at 80°C, 100% RH
5. Water absorption	<0.5 %wt at 20°C/100% RH
6. Resistance to thermal oxidation	Stable up to 85°C
7. UV absorption degradation	None at wavelength>350 nm
8. Mechanical creep	None at 90°C
9. Tensile modulus as measured by the initial slop of a stress-strain curve	<20.7 MPa (<3 kpsi) at 25°C
10. Odor, human hazards (toxicity)	None

PV modules manufacturers in Thailand have to import all amount of EVA films. The total cost of PV modules and installations are higher than other electricity sources. Thus, if we can produce EVA films for PV modules encapsulation using domestic materials and technology, it will reduce cost and expand our technology in PV modules encapsulant processing. The trends of development in PV industries are focused on the increasing efficiency of silicon solar cells and the improvement of processing. The lacks of knowledge and production technologies are important problems to develop PV industries in Thailand. However, Thailand petrochemical productions have potential to provide EVA resins for PV modules encapsulant production. To overcome these problems, the research involves the investigation and development of EVA-based encapsulant for PV modules is necessary to progress.

The commercial EVA films are made from EVA which contains 33 %wt vinyl acetate (VA) content (Elvax 150™, DuPont) and some manufacturers use EVA 28 %wt VA content. However, the domestic EVA resins in Thailand have high vinyl acetate contents up to 28 %wt. Thus, it is practically possible to use this domestic EVA to produce an EVA-based encapsulant. The study and development of EVA-based encapsulant using domestic EVA resin is feasible. The properties of the in-house encapsulant have to meet the encapsulant's specification as well.

1.2 Objectives

1. To investigate the knowledge of encapsulation materials for PV modules.
2. To develop EVA-based encapsulant using domestic raw materials for the purpose of cost reduction.

1.3 Scopes of the study

1. Study and develop the suitable formula for domestic EVA-based encapsulant.
2. Determine the significant physical properties of domestic EVA-based encapsulant.
3. Determine the crosslinking reaction and its parameters.

1.4 Research methodology

1. Study formulations, properties and processing of widely used EVA-based encapsulant.
2. Literature reviews.
3. Compound and produce EVA film using domestic EVA resins.
4. Determine the crosslinking characteristics and its parameters.
5. Modify the formula of domestic EVA-based encapsulant.
6. Determine the significant physical and chemical properties of domestic EVA-based encapsulant.
7. Conclude the results and write a report.

1.5 Outcomes of this work

1. The suitable formula for domestic EVA-based encapsulant for PV modules.
2. The EVA film which reaches the encapsulation materials requirements.

Chapter 2

Theory and Literature Reviews

2.1 Ethylene vinyl acetate copolymer [6-7]

Ethylene vinyl acetate (EVA) copolymers are characterized by the structure shown in Figure 2.1. These copolymers randomly consist of ethylene monomers and vinyl acetate monomers. EVA copolymers typically contain between 3 %wt and 40 %wt vinyl acetate contents. The low vinyl acetate content copolymers possess properties closely related to those of low density polyethylene. The higher vinyl acetate copolymers look more like gum rubber.

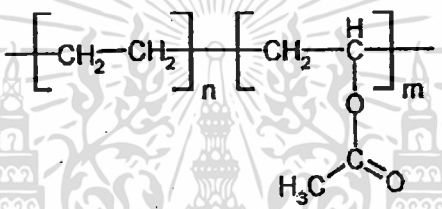

Figure 2.1 Structure of Ethylene vinyl acetate copolymer.

EVA copolymers have low crystallinity because the acetate branches interfere with crystallization. These resins are characterized by increased flexibility and resilience over a wide temperature range and by improved clarity.

The properties of EVA copolymers are defined by the comonomer content and the melt flow index (MFI). Increment of vinyl acetate contents increase flexibility, impact strength, low temperature properties and filler acceptance as well as adhesion, on the other hand it decreases crystallinity and melting point. Reducing the molecular weight of EVA copolymers increase MFI and wettability, conversely the mechanical properties and hardness are dropped [6].

Accelerated tests have shown that EVA copolymers resist degradation by weathering better than conventional polyethylene. However, chemical resistance and barrier properties of EVA copolymers are inferior. EVA copolymers accept high degrees of filler loading without serious degradation of their physical properties.

In general, EVA copolymers are used in areas where flexibility, resilience, clarity, toughness, compatibility, and excellent adhesion on various substrates. The applications are packing films and sheets which can be coextruded and laminated, injection-molded items include

shoe soles, small appliance bumpers, canister gaskets, and automobile mud flaps. Moreover, EVA copolymers are used for wax blending and adhesives [7].

2.2 EVA-based encapsulant formulations and processing [4-5]

2.2.1 EVA-based encapsulant formulations

EVA is the most commonly used for encapsulant material because of their appropriate properties that mentioned above. The formulations of EVA-based encapsulant are developed by Springborn Laboratoties, USA [4-5]. The main compositions can be divided into three groups: the EVA resins, curing agent (i.e. organic peroxide) and other additives. Table 2.1 shows the composition of Springborn Laboratoties' A9918P and 15295P formulations. A9918P is the standard cure grade, which used dialkyl peroxide type as curing agent, which has cure time approximately 25 minutes. The fast cure grade 15295P used peroxyester peroxide type which can be cured in 7 minutes. Other additives are UV absorber, UV stabilizer, antioxidant and silane coupling agent.

Table 2.1 Springborn Laboratoties' A9918P and 15295P formulations [5]

Composition	Parts [phr]
Ethylene vinyl acetate copolymer (*EVA*)	100
2,5-Bis(tert-butyldioxy)-2,5-dimethyhexane (*peroxide*) for A9918P	1.50
OO-t-Butyl-*O*-(2-ethylhexyl)-mono-percarbonate(*peroxide*) for 15295P	1.50
2-Hydroxy-4-octoxybenzophenone (*UVA*)	0.30
Bis(2,2,6,6-tetramethyl-4-piperidinyl) sebacate (*HALS*)	0.10
Tris(Nonylphenyl)phosphite (*Antioxidant*)	0.20
γ-methacryloxypropyl trimethoxy silane (*silane*)	0.25

2.2.2 EVA encapsulant processing

The encapsulant is made by first mixing EVA pellets with the ingredients and then compounded using extruder as uncured sheets at a die temperature that is low enough to preclude initiating the curing reaction (i.e. crosslinking reactions). Figure 2.2 shows the flow chart of the EVA sheet encapsulant processing. The typical thickness of an extruded, uncured EVA sheet is about 0.46 mm (18 mils). These uncured EVA sheet must store in the controlled

condition room to prevent the self-decomposition of curing agents. Then laminating and curing this encapsulant using the vacuum lamination machine with temperature 150-160°C. The curing time depends on curing agent decomposition temperature. No bubbles formed during these processes are required.

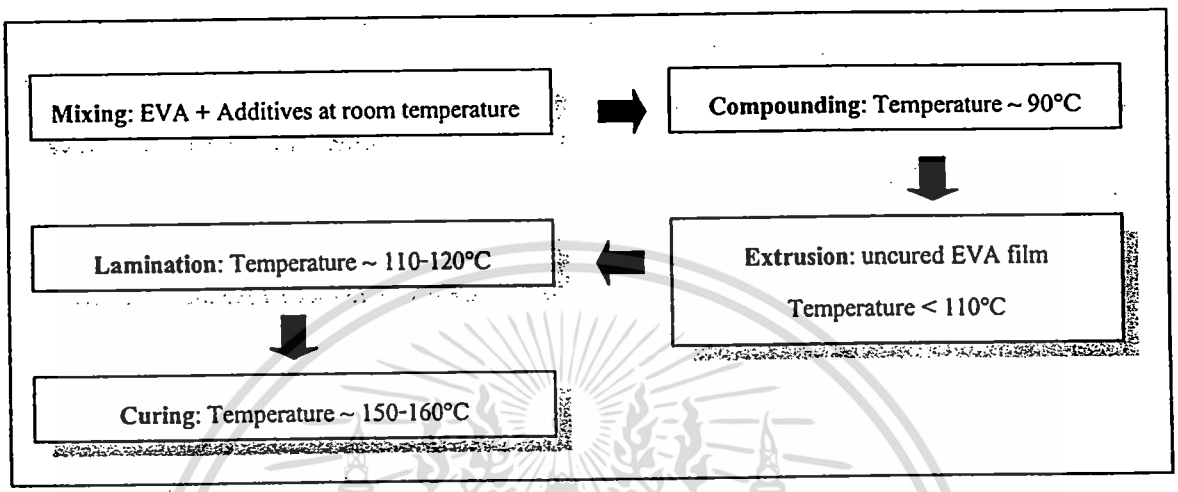

Figure 2.2 Flow chart of EVA sheet encapsulant processing.

2.3 Organic peroxides [8-10]

2.3.1 Organic peroxide compounds

Organic peroxides are compounds that possess one or more oxygen-oxygen (R-OO-R) bond. The organic peroxide general formula is:

$$R^1-O-O-R^2 \quad \text{or} \quad R^1-O-O-R^3-O-O-R^2$$

where R^1 and R^2 can be aryl, alkyl or acyl groups and R^3 can be aryl, alkyl or eater groups.

Organic peroxides are acting as free radical source. Their thermal decomposition generates very active peroxy free radicals capable to abstract hydrogen atom from the polymer backbone, particularly for polymer containing aliphatic CH_2 units. The macroradicals can then recombine to create branching and crosslinking.

There are seven major classes of organic peroxides: diacyl peroxides, peroxydicarbontes, peroxyesters, peroxyketals, dialkyl peroxides, hydroperoxides and ketone peroxides [8-9].

The use of organic peroxides can be broken down into three categories:

- Polymerization of plastic materials and polymer modification.
- Crosslinking of rubber and polyethylene.
- Curing of unsaturated polyester resins.

2.3.2 General peroxide selection

To find application in the crosslinking of polymers, organic peroxide must satisfy the following conditions [10]:

- It must be safe to handle during transportation, storage and processing.
- It must be compatible with the polymer to facilitate dispersion.
- It must be stable enough to avoid premature crosslinking at compounding temperature.
- The peroxide and its decomposition products must be non-toxic and meet the requirement of industrial hygiene.
- It should react in such a way that the crosslinking is the only modification to the polymer that occurs.

The important considerations when selecting organic peroxide for crosslinking reaction are active oxygen content, half-life temperature, minimum cure time, SADT (Self Accelerating Decomposition Temperature), maximum storage temperature and free radical energies.

2.3.2.1 Active oxygen content

Organic peroxide contains a certain amount of active oxygen which is generally between 2 and 12%. This is a good indication of the expected activity of peroxides of the same family. It is defined as the percentage ratio between the atomic mass of oxygen in each O-O bond and the molecular weight of the peroxide.

For example, Dicumyl peroxide (DCP) has one O-O group and a molar mass of 270.37; its peroxide content is 40%, so its active oxygen content will be:

$$\frac{1\times16}{270.37}\times0.40\times100=2.37\%$$

The molecular weight of oxygen is 16. The most common analytical method used for its determination is iodometric.

2.3.2.2 Half-life temperature

The half life of peroxide at any specified temperature is the time required at that temperature to affect a loss of one half of the peroxide's active oxygen content. Because the efficiency of a free radical initiator depends primarily on its rate of thermal decomposition, half-life data is essential for selecting the optimum initiator for the specific time-temperature applications. Peroxides half-life data are generated by studying their thermal decomposition in various solvents at low concentrations. In general, this half-life data is useful to express this stability in terms of 1 minute, 1 hour and 10 hours half-life temperatures, i.e., the temperatures at which 50% of the initiator has decomposed in 1 minute, 1 hour and 10 hours, respectively. In a crosslinking application, the loss of peroxide coincides with gains in C-C linkages.

2.3.2.3 Minimum cure time

When crosslinking polymers, it is important to adjust the time-temperature profile to ensure ten half-lives of peroxide decomposition. One half-life of peroxide decomposition results in 50% of the original peroxide decomposing. This would relate to a t_c50 [min] on a rheometer cure curve or the time to attain 50% of the final cure. t_c90 [min] relates to approximately four half-lives of peroxide decomposition, wherein approximately 90% of the peroxide is decomposed. The minimum cure time for crosslinking operations should be10 times of the half-life time.

2.3.2.4 Self accelerating decomposition temperature (SADT)

SADT is the lowest temperature at which peroxides in its largest shipping container undergoes self accelerating decomposition. One should know this temperature and respect it. This test is carried out in a large, temperature-controlled oven over seven days, and looks for any activity in the peroxide. If nothing happens in seven days, then the test is repeated at temperatures five degrees higher. If the peroxide undergoes a noticeable decomposition within seven days, the temperature is dropped five degrees.

2.3.2.5 Maximum storage temperature (MST)

This maximum storage temperature at which a peroxide should be stored ensures that no significant loss in peroxide assay occurs in six months. The MST is related to the quality of the product and the process. Room temperature is the primary requirement for peroxide used in the polymer crosslinking industry.

2.3.2.6 Energy of peroxide free radicals

Peroxides generate free radicals. The types of free radicals, their energy level, and the half-life of the peroxide itself are very important considerations when choosing a peroxide for a crosslinking, polymer modification, or grafting operation. Free radicals produced peroxides can have different energy level, which affects peroxide performance when crosslinking by hydrogen abstraction versus addition to a double bond. A list of hydrogen bond dissociation energies for various radical fragment precursors is provided in Table 2.2.

Table 2.2 Bond Dissociation Energies (BDE) [9]

Precursor	BDE [kJ/mol]	Description
$(R)_3C-H$	381.2	More stable, weak radicals
$(R)_2CH-H$	405.8	Poor hydrogen abstractors
RCH_2-H	418.2	More discriminate
CH_3-H	439.1	Good hydrogen abstractors
$RO-H$	439.1	Less discriminate
$R-\overset{\overset{O}{\|\|}}{C}-OO-H$	443.9	Stronger radicals
C_6H_5-H	469.0	Less stable

Peroxide radical fragments with energies less than 418.4 kJ/mol are more stable, weak radicals but are more discriminating in their reactions. Peroxides that generate these types of radicals provide good activity/selectivity with unsaturation. Radicals with energies greater than 100 kcal/mol are stronger, less discriminating, but provide good crosslinking efficiency because of hydrogen abstraction capabilities.

2.4 Silane coupling agents [11]

Silane coupling agents are silicon-based chemicals that contain two types of reactivity (inorganic and organic) in the same molecule. A typical general structure is

$$(RO)_3Si-X$$

Where RO is an alkoxy group, such as methoxy, ethoxy, or acetoxy, and X is an organofunctional group, such as amino, methacryloxy, epoxy, etc.

A silane coupling agent will act at an interface between an inorganic substrate (such as glass, metal or mineral) and an organic material (such as an organic polymer, coating or adhesive) to bond, or couple, the two dissimilar materials. A simplified picture of the coupling mechanism is shown in Figure 2.3.

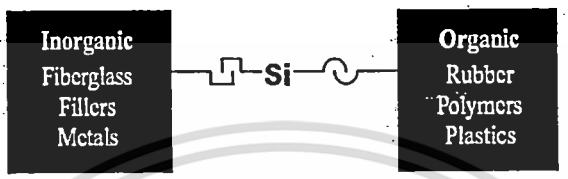

Figure 2.3 The silane coupling mechanism [11].

When organic polymers are reinforced with glass fibers or mineral, the interface, or the interphase region between the polymer and the inorganic substrate is involved in a complex interplay of physical and chemical factors. These factors are related to adhesive, physical strength, coefficient of expansion, concentration gradients and retention of product properties. A very destructive force affecting adhesion is migration of water to the hydrophilic surface of the inorganic reinforcement. Water attacks the interface destroying the bond between the polymer and reinforcement but a true coupling agent creates a water-resistant bond at the interface between the inorganic and organic materials. Silane coupling agents have the unique chemical and physical properties not only to enhance bond strength but also, more importantly, to prevent de-bonding at the interface during composite and use. The coupling agent provides a stable bond between two otherwise poorly bonding surfaces. In composites, a substantial increase in flexural strength is possible through the use of the right silane coupling agent. Silane coupling agents also increase the bond strength of coatings and adhesives as well as their resistance to humidity and other adverse environment conditions.

Other benefits silane coupling agents can provide include:

- Better wetting of inorganic substrates
- Lower viscosities during compounding
- Smoother surfaces of composites
- Less catalyst inhibition of thermoset composites
- Clearer reinforced plastics

2.4.1 Silane bond to inorganic substrate

Silane coupling agents that contain three inorganic reactive groups on silicon (usually methoxy, ethoxy or acetoxy) will bond well to the metal hydroxyl groups on most inorganic substrates, especially if the substrate contains silicon, aluminum or a heavy metal in its structure. The alkoxy groups on silicon hydrolyze to silanols, either through the addition of water or from residual water on the inorganic surface. Then the silanols coordinate with metal hydroxyl groups on the inorganic surface to form an oxane bond, so called siloxane (Si-O-Si bond) and eliminate water. It is demonstrated in Figure 2.4 and 2.5.

Silane molecules also react with each other to give a multimolecular structure of bound silane coupling agent on the surface. More than one layer or monolayer equivalents of silane is usually applied to the surface. This results in a tight siloxane network close to the inorganic surface that becomes more diffuse away from the surface.

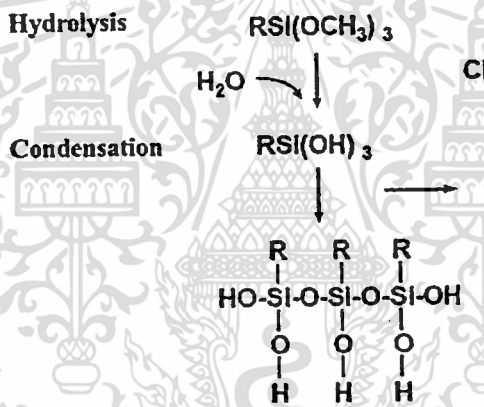

Figure 2.4 Hydrolysis of alkoxysilanes [11].

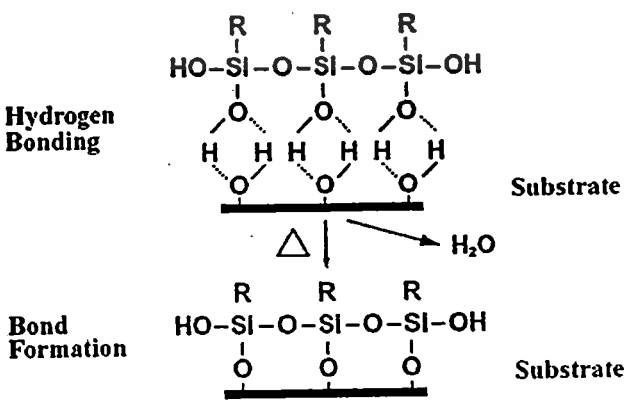

Figure 2.5 Silane coupling agent bond to an inorganic surface [11].

2.4.2 Silane bond to polymer

The bond to the organic polymer is complex. The reactivity of a thermoset polymer should be matched to the reactivity of the silane. For example, an epoxysilane to aminosilane will bond to an epoxy resin; an aminosilane will bond to a phenolic resin; and a methacrylatesilane will bond through styrene crosslinking to an unsaturated polyester resin. With thermoplastic polymers, bonding through a silane coupling agent can be explained by inter-diffusion and inter-penetrating network (IPN) formation in the interphase region as shown in Figure 2.6.

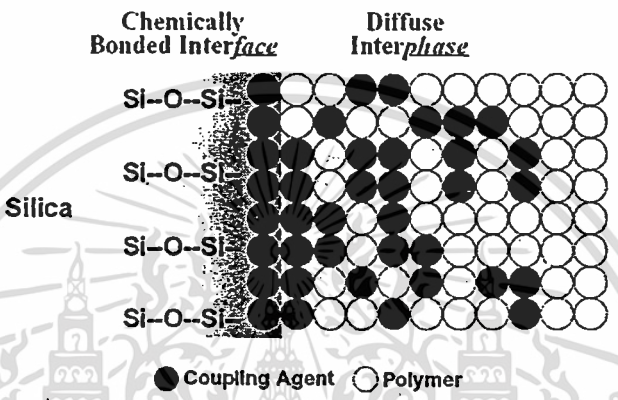

Figure 2.6 The inter-penetrating network (INP) bonding structure [11].

The ease of processing and the simple equipment required make the preferred method of producing crosslinked ethylene polymer and copolymers. The process also allows crosslinking to be delayed until after grafted product is transformed into its final product configuration. Using the same silanes, it is also possible to copolymerize the vinyl silane with ethylene monomer to make trialkoxysilyl- functionalized polyethylene. This then can be crosslinked in the same manner as the graft version.

Silane-crosslinked polyethylene is used for electrical wire and cable insulation and jacketing where ease of processing, increased temperature resistance, abrasion resistance, stress-crack resistance, improved low-temperature properties and retention of electrical properties are needed. Other applications for this technology include:

- Cold- and hot-water pipe where resistance to long-term pressure at elevated temperature is essential and natural gas pipe with good resistance to stress cracking
- Foam for insulation and packing with greater resiliency and heat resistance
- Other product and process types, such as film, blow-molded articles, sheeting and thermoforming

2.5 Crosslinking reaction mechanisms

2.5.1 Free radical polymerization [12]

The basic steps in free radical polymerization are initiation, propagation, chain transfer, and termination [12].

Initiation

Initiation can be achieved by adding a small amount of a chemical that decomposes easily to form free radicals. Initiators can be monofunctional and form the same radical or they can be multifunctional and form different radicals.

$$I_2 \xrightarrow{k_0} 2I \tag{2-1}$$

For monofunctional initiators the reaction sequence between monomer M and initiator I is

$$I + M \xrightarrow{k_i} R_1 \tag{2-2}$$

Propagation

The propagation sequence between a free radical R_1 with a monomer unit is

$$R_j + M \xrightarrow{k_p} R_{j+1} \tag{2-3}$$

The specific reaction rates k_p are assumed to be identical for the addition of each monomer to the growing chain. This is usually an excellent assumption once two or more monomers have been added to R_1. The specific reaction rate k_i is often taken to be equal to k_p.

Chain transfer

The transfer of a radical from a growing polymer chain can occur in the following ways:

1. Transfer to a monomer:

$$R_j + M \xrightarrow{k_m} P_j + R_1 \tag{2-4}$$

Here a *live* polymer chain of j monomer units transfer (R_j) its free radical to the monomer to form the radical R_1 and a *dead* polymer chain of j monomer units (P_j).

2. Transfer to another species:

$$R_j + C \xrightarrow{k_c} P_j + R_1 \tag{2-5}$$

3. Transfer of the radical to the solvent:

$$R_j + S \xrightarrow{k_s} P_j + R_1 \tag{2-6}$$

The specific reaction rates in chain transfer are all assumed to be independent of the chain length. It also notes that while the radicals R_1 produced in each of the chain transfer steps are different, they function in essentially the same manner as the radical R_1 in the propagation step to form radical R_2.

Termination

Termination to form dead polymer occurs primarily by two mechanisms:

1. Addition (coupling) of two growing polymers:

$$R_j + R_k \xrightarrow{k_{ta}} P_{j+k} \tag{2-7}$$

2. Termination by disproportionation:

$$R_j + R_k \xrightarrow{k_{td}} P_j + P_k \tag{2-8}$$

2.5.2 Organic peroxide crosslinking reaction [8-9, 13-14]

Crosslinking reaction starts at high temperatures, and it brings to the formation of a three dimensional network by creating bonds between the polymer chains. Peroxide crosslinking may happen typically in a temperature range varying from 110 to more than 200°C and leads to carbon-to-carbon bonds creation by hydrogen abstraction from the polymer chain. Mishra et al. [14] summarized the scheme of the crosslinking reaction initiated by the thermal decomposition of organic peroxide can be given in the following form:

Step 1: Thermal decomposition of organic peroxide

Organic peroxides can be decomposed by thermal decomposition reaction. One molecule of peroxide produces two or more free radicals (RO*). These free radicals are initiator of crosslinking reaction.

$$\text{R-O-O-R} \xrightarrow{k_0} 2\,(\text{RO}^*) \tag{2-9}$$

Step 2: Hydrogen abstraction with radical formation on the polymer chain (Initiation)

Free radicals react to hydrogen atom on polymer chain by hydrogen abstraction to produce the free macroradical ($[CH_2HC^*]_n$) and generate alkyl alcohol (R-OH) as by product.

$$\text{RO}^* + \left[CH_2CH_2\right]_n \xrightarrow{k_i} \left[CH_2HC^*\right]_n + \text{R-OH} \tag{2-10}$$

Step 3: Crosslinking reaction by macro free radical recombination (Propagation)

Recombination of free macroradicals causes the crosslinked polymer chains. The crosslinking reaction creates the three dimension network of polymer bulk. The C-C bonds are rigid structure which increases the mechanical properties of crosslinked polymer.

$$\left[CH_2HC^*\right]_n + \left[^*CHCH_2\right]_m \xrightarrow{k_p} \left[CH_2HC\right]_n - \left[CHCH_2\right]_m \tag{2-11}$$

Furthermore, free radicals can be disproportionate to produce other types of free radicals, so-called the secondary free radicals, or by-products. Then the secondary free radicals itself step towards the propagation and termination, respectively.

Four classes of organic peroxides are use commercially for crosslinking and polymer modification [8-9] including diacyl, peroxyester, peroxyketal and dialkyl peroxides. The most common peroxide used in the crosslinking industry has traditional been the dialkyl class.

Thaworn et al. [13] illustrated the mechanism of EVA crosslinking reaction with Dicumyl peroxide (DCP, dialkyl class) as shown in Figure 2.7.

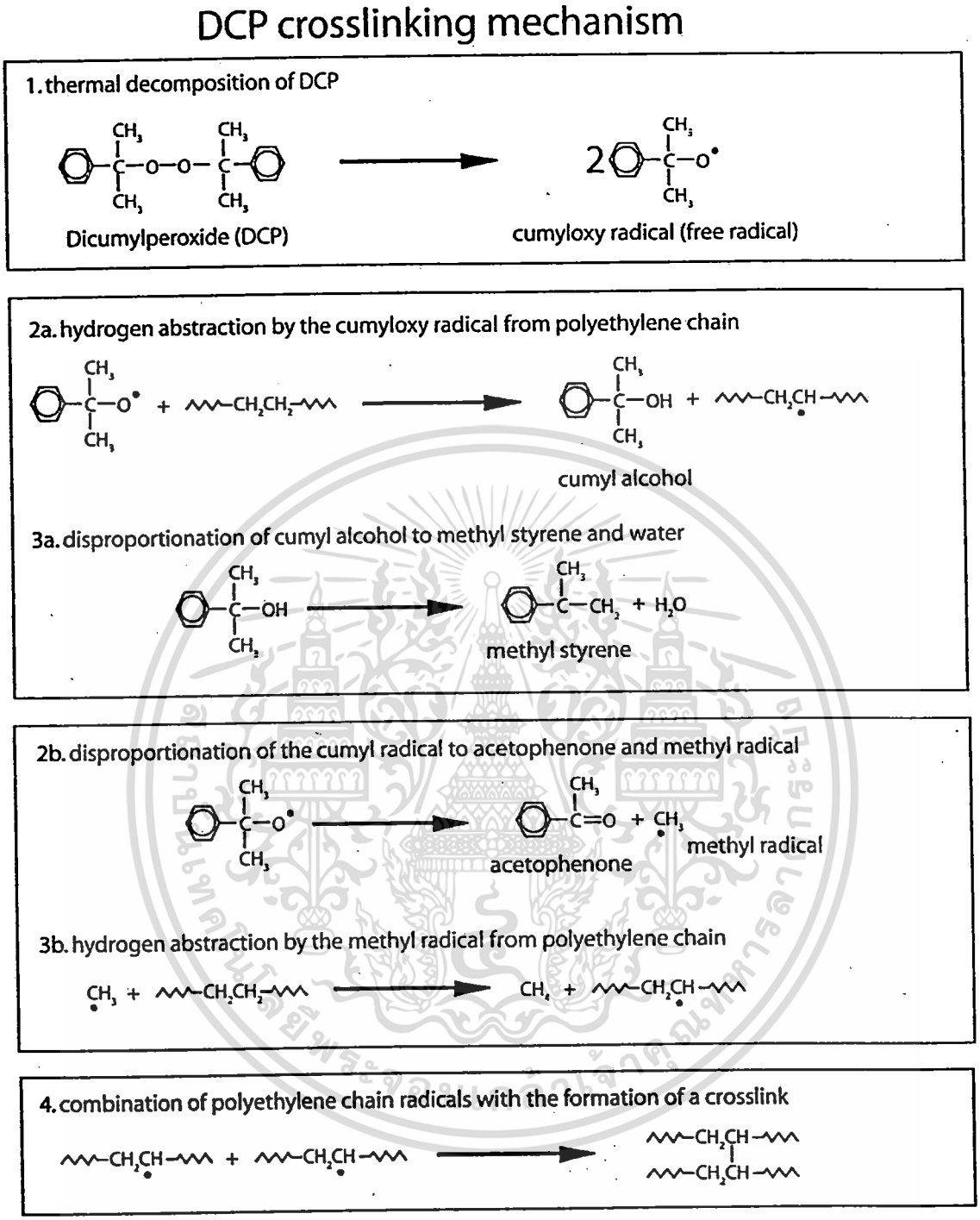

Figure 2.7 Crosslinking with organic peroxide mechanism [13].

2.5.3 Silane Crosslinking Reaction [11, 13, 15-16]

Although polymers such as EVA are readily crosslinked by treatment with organic peroxides, the moisture curing of silane crosslinking provides unique advantage in terms of processing and product quality. The dimensional accuracy of moisture curing is superior to peroxide-based processes and the density of the crosslinked product is generally higher. Moreover, the structure of siloxane bridges (Si-O-Si bond) is less rigid than C-C bonds and gives flexibility to the crosslinked polymers. J. S. Parent et al. [15] and V. Bounor-Legaré et al. [16] suggested that the crosslinking can take place either in two steps (i.e. grafting and then moisture crosslinking) or through a simultaneous exchange between two alkoxide groups of one silane molecule with two pendant ester groups belonging to two different EVA chains. The limitation of the collision probability between ester groups of EVA and silane as the crosslinking density increases may contribute to decrease the speed of the reaction and so to reach the observed plateau on conversion-time curve.

The two major reactions occur during the silane crosslinking are:

1. Grafting reaction (Propagation)

There are two general sites for macroradical generation; one is on the main chain of the polymer and another site is on the pendant ester groups. For EVA, it can be generated macroradicals on ethylene main chain and acetyl groups via the peroxide thermal decomposition and propagation. On the main chain radical site, there are four expected modes of reactivity: silane grafting, disproportionation (to introduce unsaturation), combination (to introduce crosslinking), and β-scission. Another radical site on the acetyl group has its expected reactivity modes reduced to only silane grafting or combination.

2. Moisture crosslinking reaction (Termination)

The grafted polymer main chain and the grafted pendent ester groups are crosslinked in the presence of water (moisture crosslinking) generally catalyzed by tin compound as a precursor or other suitable catalysts. In addition, there are well-suited silanes without precursor required for moisture crosslinking. It depends on conditions of crosslinking process.

For example, the mechanisms of EVA crosslinked with g-methacryloxy propyl trimethoxysilane as already explained in a previous study [13] shown in Figure 2.8.

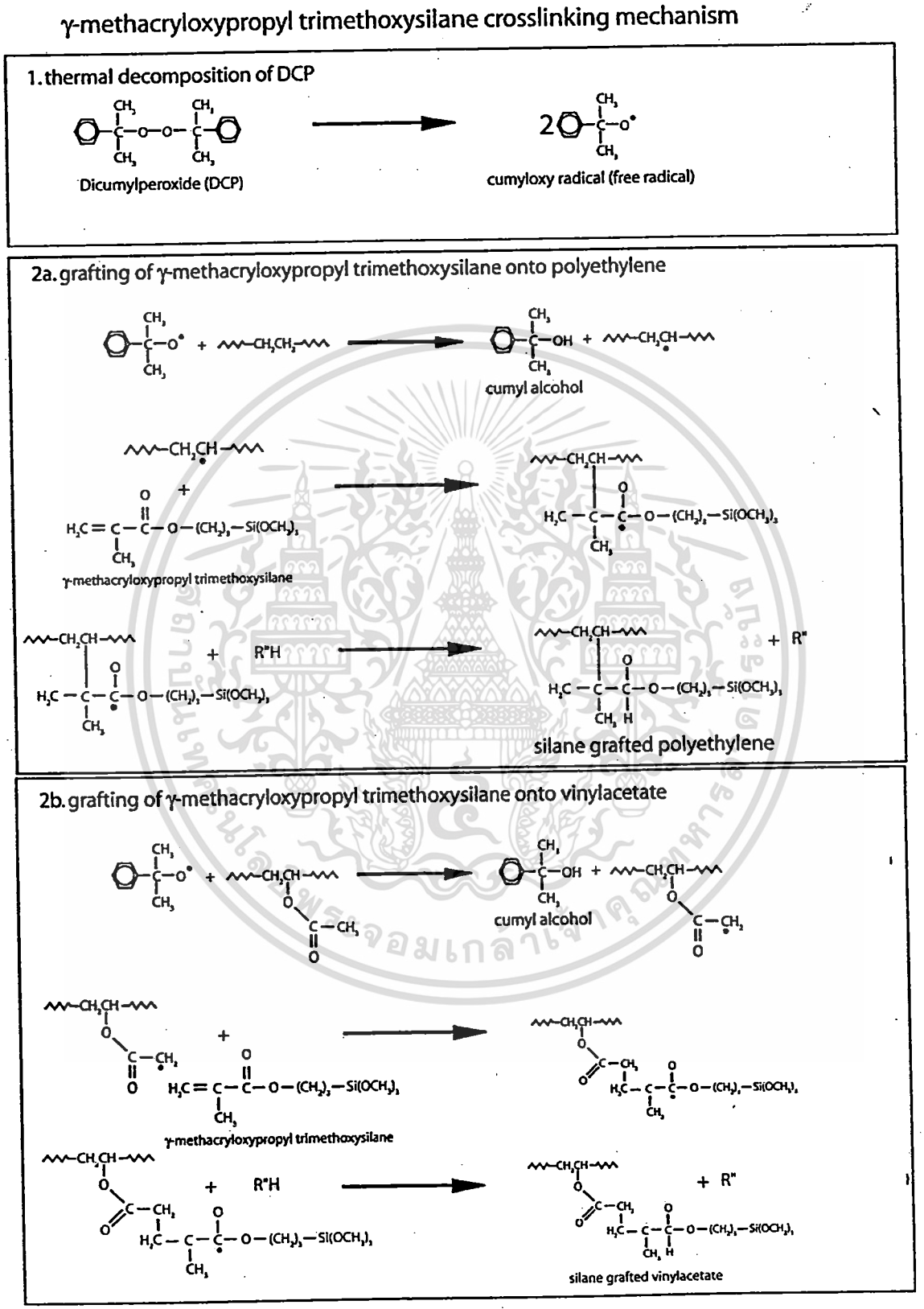

Figure 2.8 Crosslinking with silane coupling agent mechanism [13].

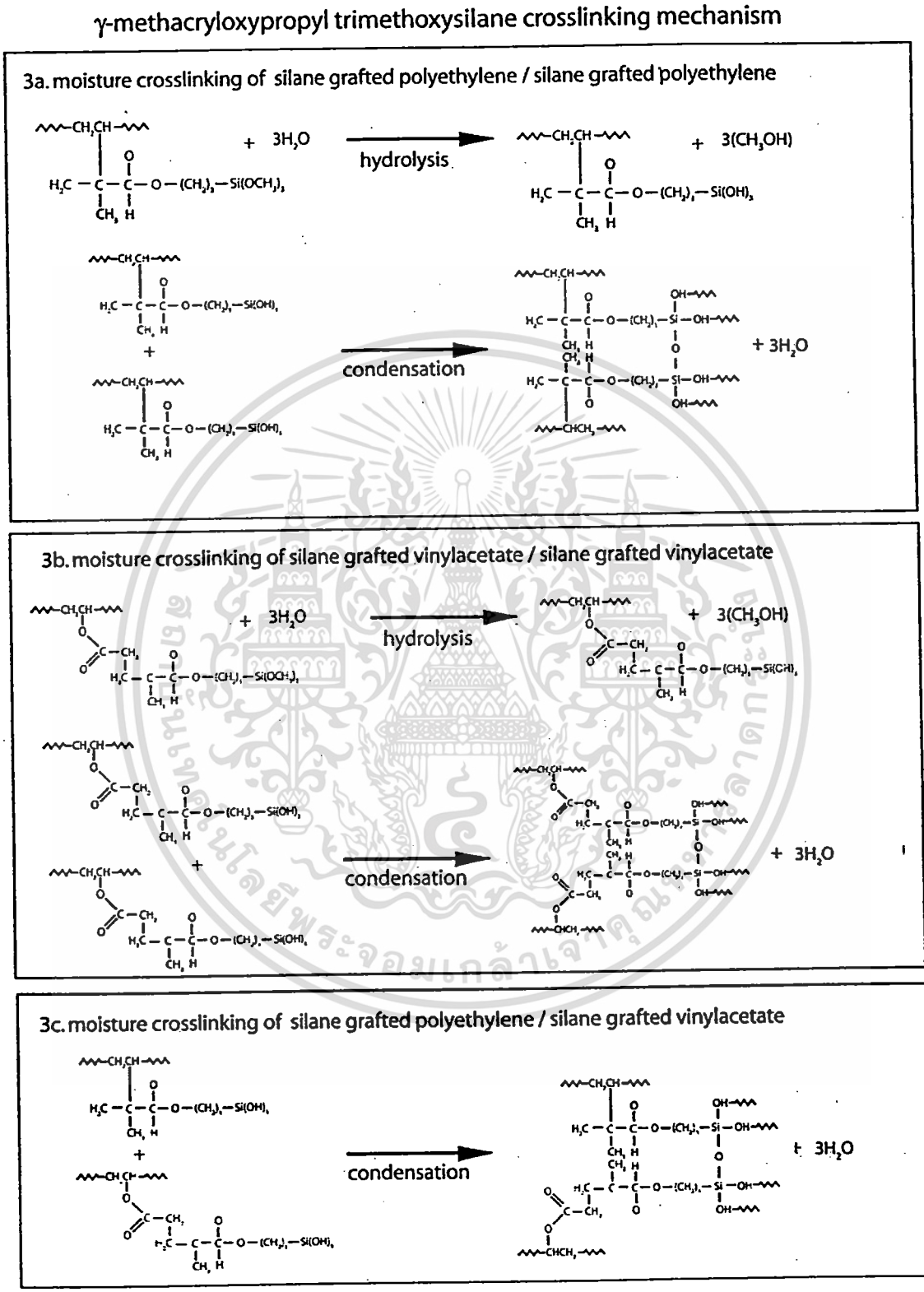

Figure 2.8 (cont.) Crosslinking with silane coupling agent mechanism [13].

2.6 Crosslinking characteristics [9, 17-19]

2.6.1 Moving die rheometer (MDR)

The curemeter is one of the most versatile equipment for researcher and development, production control and quality control work on polymeric materials. It is a laboratory tool often used to predict processing behavior and to simulate realistic-use conditions. The Oscillating Disc Rheometer (ODR) is one type of curemeters. ODR machines establish the change in compound stiffness by monitoring the change in torque when shearing a polymer sample between a biconical disc and an accurately temperature-controlled cavity. The concept of a rotational test was carry-over from the Mooney-type machine (a rotational shearing-disc viscometer), and a full cure curve can be obtained due to oscillatory movement of the disc. Even though ODRs have been used worldwide, the ODR itself has a design flaw which involves the use of the ODR disc itself. The heat sink of ODR disc and poor quality of torque signals measured through the shaft of the rotor as well as the lack of barrier film using are major problems. These problems were greatly reduced with the introduction of new rotorless curemeters such as the Moving Die Rheometer [9, 17].

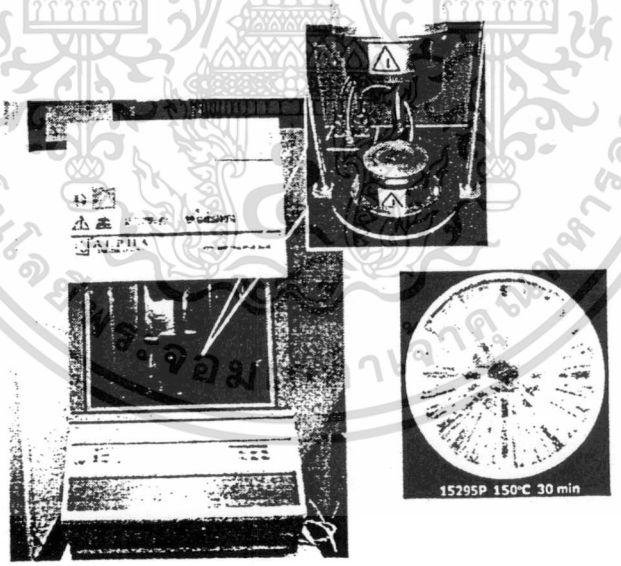

Figure 2.9 Moving Die Rheometer (MDR) model MDR 2000 (Alpha Techonologies).

In a MDR instrument, the lower die oscillates sinusoidally, applying a strain to the specimen which is contained within a sealed, pressurized cavity. The upper die is attached to a reaction torque transducer which measures the torque response. This design greatly improves the test sensitivity measurement so that real changes in a compound can be detected faster. Also,

because there is no rotor, the temperature recovery of the test specimen is less than 30 seconds, compared to approximately 4 to 5 minutes for the older ODR design. Moreover, barrier film can be used with rotorless curemeters which greatly reduces clean-up time.

With the MDR according to ASTM D 5289 [9, 18-19], two curves are produced during cure. The elastic torque (S') is the traditional cure curve which is more commonly used as an indication of cure state. The formation of crosslinks from the vulcanization process causes elastic torque to rise. The viscous torque (S'') curve is a second curve generated simultaneously. This relates to the pure flow characteristics of the polymer and commonly uses to calculate real dynamic viscosity.

Figure 2.10 shows the typical cure curves of elastic torque including plateau, reversion and marching types. The curve in Figure 2.10a represents a cure that forms a perfect plateau. The compound in this category reaches the ultimate state of cure (ultimate crosslink density). The curve in Figure 2.10b illustrates the reversion cure. Natural rubber formulations are one example of compounds that will revert if the cure temperature is high enough. Lastly, Figure 2.10c shows a curve that marches or has marching modulus. It continuously increases in hardness and never does fully plateau. Hereby M_L is the minimum torque while M_{HF}, M_{HR} and M_H are the maximum torque of cure that plateaus, reverts and marches, respectively.

2.6.2 Cure time

Cure time refers to the amount of time required to reach specified states of cure at a specified cure temperature. The t_Cx is simply the time to reach a given percent x state of cure which is illustrated in Figure 2.11. The t_Cx is calculated as follows:

$$t_C\text{x is the time to produce torque } (\tau) = (\text{x}/100) \bullet (M_H - M_L) + M_L \qquad (2\text{-}12)$$

Where M_L = minimum torque [dN•m]

M_H = maximum torque [dN•m]

x = percent state of cure

t_Cx = time to a given percent (x) state of cure

For example, t_C90 is time required to reach 90% of the state of cure.

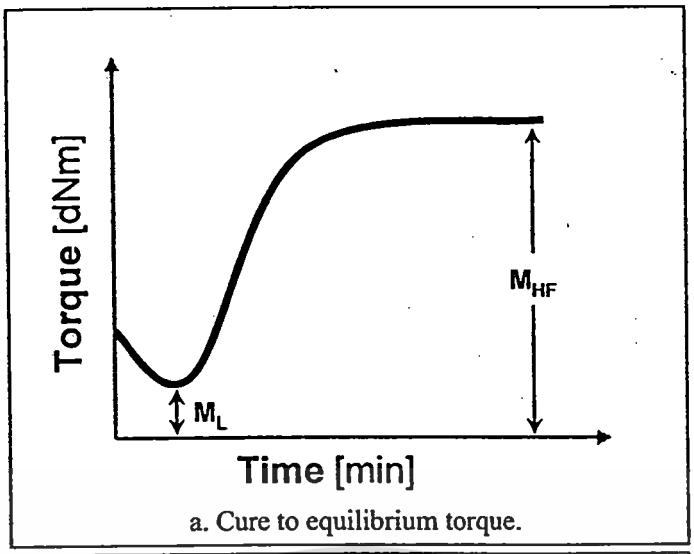

a. Cure to equilibrium torque.

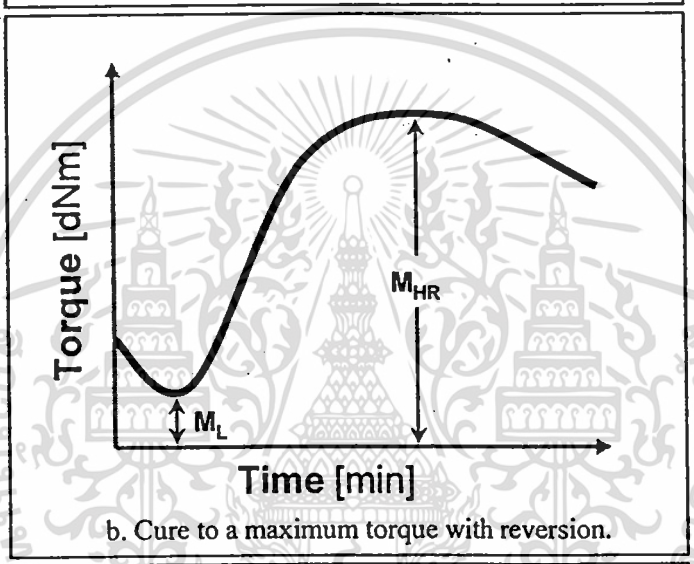

b. Cure to a maximum torque with reversion.

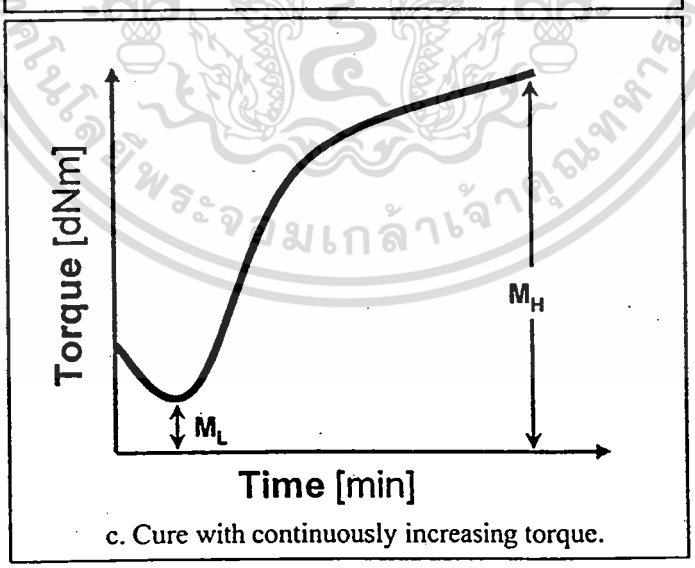

c. Cure with continuously increasing torque.

Figure 2.10 Typical cure curves of elastic torque.

a. Cure to equilibrium torque;

b. Cure to a maximum torque with reversion;

c. Cure with continuously increasing torque.

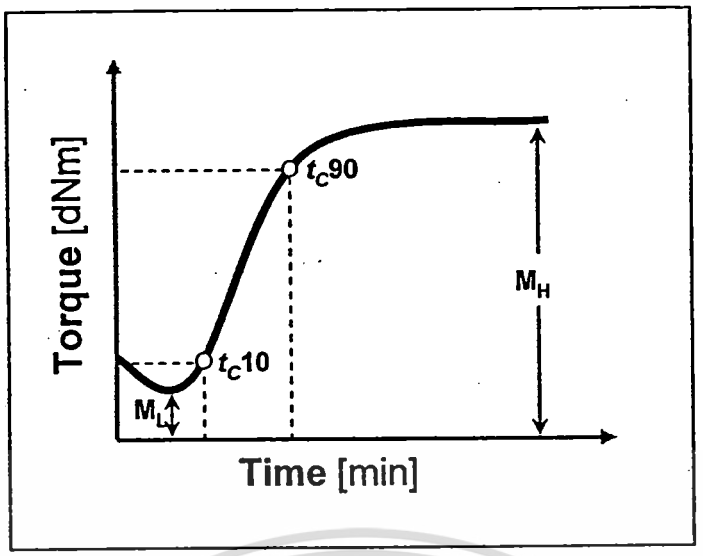

Figure 2.11 Illustration of the calculation of t_C10 and t_C90.

2.6.3 Cure rate

Cure rate is the speed at which a compound increases in modulus (crosslinking density) at a specified cure temperature. The maximum cure rate is the slope of the tangent line at the inflection point on the cure curve while the Cure Rate Index is calculated as follows:

$$\text{Cure Rate Index} = 100 / (\text{Cure Time} - \text{Scorch Time}) \quad (2\text{-}13)$$

The use of this index can select preferred cure and scorch times, such as t_C90 and t_S1.

MDR scorch time is usually defined as the time until one torque unit rise above the minimum is achieved (t_S1) when 1° arc strain is applied. Also, through the computer software used today with MDR, it is relatively easy to calculate time to 10% state-of-cure (t_C10). This cure time t_C10 also relates to scorch. The parameter t_C10 may have an advantage over t_S1 because it is not based arbitrarily on a one torque unit rise. Hence, the Equation 2-13 can be rewritten to:

$$\text{Cure Rate Index} = 100 / (t_C90 - t_C10) \quad (2\text{-}14)$$

2.7 Isothermal Isoconversional Kinetic Analysis [12, 20-23, 39]

There is not a direct method to measure the conversion during the crosslinking reaction occurred. The gel content measurement was used to estimate the conversion but this method used organic solvent to dissolve the crosslinked sample and took long time to operate. So, the MDR method was applied to investigate the real-time crosslinking reaction. Although this method resulted as torque-time data, these outputs did not directly relate to their conversion. Thus, Dick and Pawlowski [20] had developed an equation to estimate the conversion from cure curves data as shown in Eq. (2-15).

$$\alpha_t = \frac{C_t}{C_\infty} \cong \frac{\left(\tau_t - M_L\right)}{\left(M_H - M_L\right)} \tag{2-15}$$

where α_t = conversion at any given time

C_t = concentration of crosslinks at time t

C_∞ = final concentration of crosslinks ($t \rightarrow \infty$)

τ_t = torque at time t [dNm]

M_L = minimum torque [dNm]

M_H = maximum torque [dNm]

In general, the cure kinetic analysis of polymer [12] can be described by Eq. (2-16)

$$\frac{d\alpha}{dt} = kf(\alpha) \tag{2-16}$$

where k is the reaction rate constant, $f(\alpha)$ is the reaction model, α is the degree of conversion and t is the time. Integration the above equation gives the integral rate law as follows:

$$g(\alpha) = kt \tag{2-17}$$

where $g(\alpha)$ is the integral reaction model. These equations called the traditional model-fitting methods. The temperature dependence of the rate constant is usually described by the Arrhenius equation:

$$k = A\exp(\frac{-E_a}{RT}) \tag{2-18}$$

where A is the pre-exponential (frequency) factor, E_a is the activation energy, T is the absolute temperature and R is the gas constant. Substituting Eq. (2-18) in the above two rate expressions gives

$$\frac{d\alpha}{dt} = A\exp\left(\frac{-E_a}{RT}\right)f(\alpha) \tag{2-19}$$

$$g(\alpha) = A\exp\left(\frac{-E_a}{RT}\right)t \tag{2-20}$$

Model-fitting methods involve two fits: the first determines the model that best fit the data (Eq. (2-17)) while the second determines specific kinetic parameters such as the activation energy and frequency factor using the Arrhenius equation [21]. These methods are obviously used in kinetic analysis. However, the polymer crosslinking reactions are complex mechanisms which would not easily assume the best-fit model to describe whole reactions. So, the isoconversional (model-free) methods [21-23] were developed for calculating the activation energy. The activation energy from the model-free methods called the effective activation energy ($E_{a,eff}$) [39] as a parameter measured from a temperature dependence of the overall reaction rate.

The model-free methods calculate the effective activation energy values at progressive degrees of conversion without any modelistic assumptions. The standard model-free method is based on taking the natural logarithm of Eq. (2-20) giving

$$-\ln t_\alpha = \ln\left(\frac{A}{g(\alpha)}\right) - \frac{E_{a,eff}}{RT} \tag{2-21}$$

where t_α is time at given conversion (i.e. $t_{\alpha=0.1}$ is time at 10% conversion) and $E_{a,eff}$ is effective activation energy. A plot of $-\ln t_\alpha$ versus $1/T$ at each α (e.g. α = 0.1-0.9) yields $E_{a,eff}$ (from the

slope) for that α regardless of the model. Friedman's method [21] is based on taking the natural logarithm of Eq. (2-19) giving

$$\ln\left(\frac{d\alpha}{dt_\alpha}\right) = \ln(Af(\alpha)) - \frac{E_{a,eff}}{RT} \tag{2-22}$$

A plot of $\ln(d\alpha/dt_\alpha)$ versus $1/T$ at each α (e.g. α = 0.1-0.9) yields $E_{a,eff}$ (from the slope) for that α regardless of the model as well.

2.8 Gel content [24-25]

The gel content or insoluble fraction produced in ethylene plastics by crosslinking can be determined by extracting with solvents such as decahydronaphthalene or xylene (ASTM D 2765-90). The extraction test method was described herein. It is applicable to crosslinked ethylene plastics of all densities, including containing fillers, and all provides corrections for the inert fillers present in some of those compounds [24].

In general, specimens of the crosslinked ethylene plastic are weighed and then immersed in the extracting solvent using reflux apparatus (Figure 2.12) at the temperature specified by the procedure selected and for the time designated by that procedure (extract the specimen for 6 hours in decahydronaphthalene or for 12 hours in xylene). After extraction, the specimens are removed, dried and reweighed as directed. The amount of material extracted is calculated. The gel content can be calculated [25] by Eq. (2-23).

$$\text{Gel Content}[\%] = \left(\frac{\text{weight of undissolved content}}{\text{original weight of sample}}\right) \times 100 \tag{2-23}$$

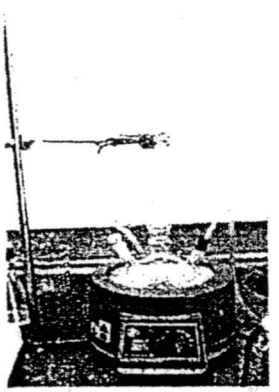

Figure 2.12 Reflux apparatus.

2.9 Light Transmission

2.9.1 Solar radiation [26-27]

Light or electromagnetic radiation can be divided into several bands or categories each defined by a specific wavelength range. Solar radiation is the naturally occurring radiation that reaches the earth's surface. It includes visible light as well as ultraviolet and infrared light as shown in Figure 2.13.

The sun emits almost all of its energy in a range of wavelength from about 200 to 4,000 nm [26]. Most of this energy is in the visible light region (400-700 nm). Each wavelength corresponds to a frequency and energy: the shorter the wavelength, the higher the frequency and the greater the energy (which is expressed in electron-volts or eV). Red light is at low-energy end of the visible spectrum and the violet light is at the high-energy end, where it has half again s much energy as red light. In the invisible portions of the spectrum, radiation in the ultraviolet region (200-400 nm), which causes the skin to tan, has more energy than that in the visible region. Likewise, radiation in the infrared region (700-2,200 nm), which we feel as heat, has less energy than the radiation in the visible region.

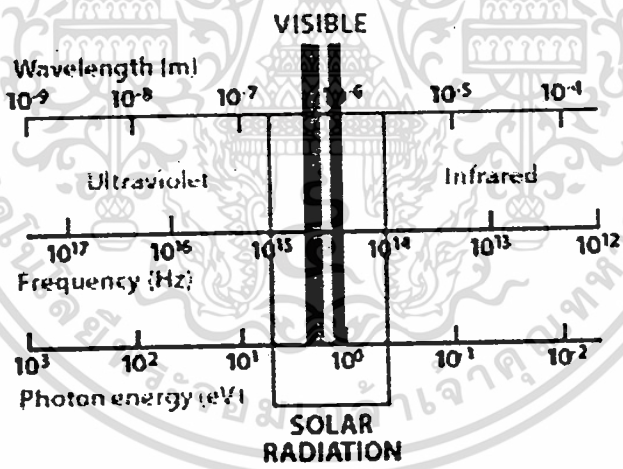

Figure 2.13 The solar radiation spectrum [26].

The intensity of the solar radiation [27] that penetrates the atmosphere and reaches the earth varies considerably, depending on the altitude, ozone levels, concentration of water vapor, carbon monoxide, dust and other types of contamination. The approximate relative distribution of solar energy at mean noon sea level sunlight presents that the ultraviolet band accounts for approximately 3% of the total solar energy, whereas the visible band accounts for 45% and the infrared band accounts for 52%.

Solar cells respond differently to the different wavelengths, or colors, of light. For example, crystalline silicon can use the entire visible spectrum, plus some part of the infrared spectrum. But energy in the part of infrared spectrum, as well as longer-wavelength radiation, is too low to produce current flow. Higher-energy radiation can produce current flow but much of this energy is likewise not usable.

2.9.2 Principles of absorption spectroscopy [4-5, 28]

The processes concerned in absorption spectroscopy are absorption and transmission. Usually the conditions under which the sample is examined are chosen to keep reflection, scatter and fluorescence to a minimum. Ultraviolet and visible spectroscopy is almost entirely used for quantitative analysis; that is the estimation of the amount of a compound known to be present in the sample. The sample is usually examined in solution. With solid sample it is usually found that the material is in a condition unsuitable for direct spectrometry. The refractive index of the material is high and a large proportion of the radiation may be lost by random reflection at the surface or in the mass. Unless the sample can be easily made as homogenous polished block or film, it is usual to eliminate these interfaces by dissolving it in a transparent solvent.

In PV lamination-packing process, the transparency or light transmission of encapsulants are considerably important because its transparency has an effect on the module's efficiency. UV-Vis spectrophotometer is quite well known for light transmission measurement of encapsulants [4-5].

Lambert's Law [28]

Lambert's Law states that each layer of equal thickness of an absorbing medium absorbs an equal fraction of the radiant energy that traverses it. The fraction of radiant energy transmitted by a given thickness of the absorbing medium is independent of the intensity of the incident radiation, provided that the radiation does not alter the physical or chemical state of the medium.

If the intensity of the incident radiation is I_0 and that of the transmitted light is I, then the fraction transmitted or so-called transmittance T is:

$$\frac{I}{I_0} = T \tag{2-23}$$

The percentage transmittance (*%T*) is:

$$\%T = \frac{I}{I_0} \times 100 \tag{2-24}$$

For example, if a series of colored glass plates of equal thickness are placed in parallel, each sheet of which absorbs one quarter of the light incident upon it, then the amount of the original radiation passed by the first sheet is (1 - ¼)/1 x 100 = 75%.

And by the second sheet is 56.25%, i.e. 75% of 75%, and by the third sheet is 42.19%, i.e. 75% of 56.25%, and by the n^{th} sheet is $(0.75)^n$ x 100%.

Beer-Lambert Law [28]

The Beer-Lambert Law states that the concentration of a substance in solution is directly proportional to the 'absorbance' of the solution following Eq. (2-24). When monochromatic radiation passes through a homogenous solution in a cell, the intensity of the emitted radiation depends upon the thickness and concentration of the solution. Absorbance in older literature is sometimes referred to as 'extinction' or 'optical density'.

$$A = \varepsilon CL \tag{2-24}$$

Where A is the absorbance, L is the length of the radiation path through the sample, ε is the extinction coefficient—a constant dependent only on the nature of the molecule and the wavelength of the radiation.

Mathematically, absorbance is related to percentage transmittance by the expressions:

$$A = \log_{10}\left(\frac{I}{I_0}\right) = \log_{10}\left(\frac{100}{T}\right) = \varepsilon CL \tag{2-25}$$

$$A = \log_{10}\left(\frac{100}{T}\right) = \log_{10} 100 - \log_{10} T = 2 - \log_{10} T \tag{2-26}$$

2.10 Literature Reviews

The correspondence articles are as follows:

The Jet Propulsion Laboratory (JPL) managed the "Flat-Plate Solar Array (FAS) Project for the United States Department of Energy. The project objective was to conducted research on photovoltaic arrays establishing their technical feasibility so then industry could meet a target price for modules of less than 70 cent per Wpk (in 1980 dollars) and with a minimum service life time of 20-30 years. Cuddihy et al. [29] noticed four encapsulant candidates including ethylene vinyl acetate (EVA), ethylene methyl acrylate (EMA), poly-n-butyl acrylate (PnBA) and aliphatic polyether urethane (PU). EVA was recommended on the basis of reasonable low cost and other requirements such as elastomeric (thermoplastic) properties, transparency, weatherability and good module processability. Furthermore, EVA was convenient for dry-film lamination method which proceeded easier than casting method. The formulation of EVA encapsulation film was developed and was initially used in the PV industry. The analyses for structure adequacy identified that the thermal expansion or wind deflection of PV modules could result in the development of mechanical stresses in the encapsulated solar cells sufficient to cause cell breakage. However, those stresses could be reduced by increasing the thickness (t, in unit of mil) or by using materials with lower Young's modulus (E, in unit of kpsi). The encapsulant ability to dampen transmitted stress was directly related to the ratio of its thickness to modulus (t/E). At a ratio of 4, the solar cell stresses were just at their allowable limit. EVA had a Young's modulus of 0.9 kpsi, and then the minimum thickness would be 4-5 mils. The use of an encapsulant having a higher Young's modulus would necessitate that the thickness of that encapsulant was correspondingly increased.

Lewis [30] summarized the requirements of encapsulant material for PV modules that the encapsulant (or a pottant in old literatures) must be high transparent (> 90% from 400 to 1,100 nm), serving as an optical coupling medium to provide maximum light transmission to the cell surface. The encapsulant must be very inexpensive (≤$ 2.15/m^2). Encapsulant material should have a relatively low modulus (≤ 2,000 psi at 25°C). The minimum usable encapsulant thickness could be limited by the green strength of the material itself. The suggested minimum thickness was about 10-15 mils (1 mil = 0.001 in) to achieve the necessary freedom from flaws for sufficient electrical insulation properties as well as ease of handling. In general, the film thickness was nominally 18 mils. The encapsulant material must have a glass transition temperature below the lowest temperature extreme the PV module might experience, which was about -40°C.

The materials must remain rubbery in order to damp impacts and vibration of the fragile cells. Moreover, it must exhibit strongly moisture-resistant adhesion (≥ 1,750 N/m of peel strength) to all the surfaces it must bond to, over a 20-years lifetime. Moisture-resistant adhesion was tested mostly by exposure to 100°C/100% RH. Ten months at these conditions would equal 20 years at 70°C/50% RH, but usually the first week or two would separate the good bond from the poor ones. Exposure to boiling water for a few hours or overnight was also a good initial screening technique. The encapsulant must be stable; that is, chemically resistant to oxidation and hydrolysis unless protected in a heretic package, to reduction by metals, and to outgassing of dissolved gasses or liquids or decomposition products under normal operating conditions of -40°C to + 90°C for 20 years. Furthermore, the encapsulant should have a dielectric strength of at least 400-500 volts/mil, which was typical for unoriented amorphous polymers. A non-softening, high volume resistivity insulator layer was thus needed to guarantee circuit isolation.

Burger and Cuddihy [31] improved the lamination process. The cure cycle used for lamination process was evacuation for 5 min, then 25 min of cure. During the 25-min cure, the first 8-10 min was required to raise the encapsulant temperature to 150°C, where it was maintained to the end of the cycle. Modules were then removed without being cooled. Modules fabricated with this cure cycle showed even and complete curing and no bubbles.

Pern [32] studied factors that might affect the net discoloration rate of the two typical EVA encapsulants (A9918 and 15295) used in crystalline-Si photovoltaic (c-Si PV) modules upon accelerated exposure. The results indicated that the rate of discoloration was affected by several factors including (1) curing agent and curing conditions; (2) presence and concentration of curing-generated, UV-excitable chromophores; (3) UV light intensity; (4) loss rate of UV absorber: (5) lamination; (6) film thickness and (7) photobleaching rate due to the diffusion of air into the laminated film. In general, the loss rate of UV absorber and the rate of discoloration from light yellow to brown followed a sigmoidal pattern. A reasonable correlation for net changes in transmittance at 420 nm, yellow index, and fluorescence peak area (or intensity) ratio was obtained as the extent of EVA discoloration progressed.

Czanderna and Pern [4] had provided an overview about encapsulation of PV cells and modules. A critical review about what is and is not known about using EVA as the encapsulant material in PV modules was determined. In addition, they elucidated the complexity of the encapsulation problem and summarized the general problems of polymer stability in a solar environment. They investigated the general degradation mechanisms of stabilized, cure EVA

through a series of simulated degradation experiments. Their results indicated that the EVA discoloration resulted primarily from the formation of polyconjugated C=C bonds (polyenes) by multistep deactylations and from the presence of α,β-unsaturated carbonyl groups. Furthermore, acetic acid that was produced by thermal and photothermal decomposition exhibited an autocatalytic effect on the EVA yellowing.

Klemchuck et al. [5] reported the Springborn Laboratories' EVA A9918P formulation which modified A9918 by adding small amount of silane coupling agent. They studied the discoloration of EVA encapsulant in field-aged solar energy modules. The discoloration had been found to be due to interactions between crosslinking peroxide and some stabilizing additives, and was also likely to be due to oxidation of the encapsulant. They suggested that reformulated encapsulant and the use of cerium-oxide-containing glass as the top cover of PV modules had dramatically reduced discoloration.

Galica and Sherman [33] developed the faster-curing and flame-retardant EVA-based encapsulant formulations and conducted an improved technique of cure kinetic measurement by using Moving Die Rheometer which could be reduced cure time determination about 70% of ordinary technique (standard gel content test).

Shea and Wohlgemuth [34] concluded that the rate of encapsulant cure might be accelerated by multiple means. High lamination temperature would dramatically reduce the curative's half-life, thereby reducing the time required to achieve an acceptable level of crosslinking. The employment of acetic acid scavengers and/or peroxide co-agents could lead to faster curing of EVA-based encapsulants at current or higher processing temperatures. Formulation of the encapsulant with a more active peroxide that had a shorter half-life versus the present OO-t-Butyl O-(2-Ethylhexyl) Monoperoxycarbonate (TBEC) curative could speed the process. Moreover, they compared the selected polymeric candidates for the faster curing encapsulant system. For screening purposes they were evaluated versus STR 15295P EVA-based encapsulant system. Those considered including a number of EVAs ranging from 10-32%wt vinyl acetate supplied by 4 different supplies; a series of ethylene butyl acrylate (EBA) copolymers ranging from 7-35%wt butyl acrylate; ethylene methyl acrylate (EMA) copolymers ranging from 10-30%wt methyl acrylate; and ethylene octene copolymers ranging from 20-28%wt octene. In conclusion, DuPont's 32%wt vinyl acetate containing EVA was found to offer the most advantage in optical properties and was generally less expensive that other alternatives identified. Based upon these measured results, it appeared that only the highest VA content EVAs had the

desired level of optical transparency for front sheet encapsulant applications. Of the other ethylene copolymers evaluated, only those of the highest copolymer contents were determined to have average light transmissions raging from 89-91%, all of which were more costly than the EVA copolymers. Furthermore, they had developed a new EVA formulation and demonstrated 6 minutes process to achieve adequate cure of PV modules in standard lamination equipment.

Likewise, Agro and Tucker [35] have improved encapsulant/packing materials for thin film PV. In this phase I, they surveyed the requirements of PV module manufactures. Device packing represented approximately one half of module production costs. Thus, lower cost packing as well as faster process and operating temperature below 200°C were needed by manufacturers.

Chapter 3

Research Methodology

This investigation of EVA-based encapsulants can be separated into 2 parts including compounding process and characterizing their essential properties such as crosslinking characteristics, cure kinetics, gel content and transparency. Three types of EVA resins were used in this experiment. The commercial grade EVA which contains 33%wt VA content and domestic EVA which contains 18 and 28 %wt VA contents were used as received. The data of these EVAs and additives were listed in Table 3.1-3.4. These EVAs were compounded with organic peroxides, silane coupling agent and additives by using twin-screw extruder and then sheeting by two-roll mill. The crosslinking characteristics were studied by a Moving Die Rheometer (MDR 2000) according to ASTM D 5289-97 and the isothermal isoconversional kinetic method was used to analyze their cure kinetics. In addition, optical property was measured by UV-Vis spectrophotometer as well as the gel content was tested following ASTM D 2765-90 method.

Table 3.1 Ethylene vinyl acetate (EVA) copolymers data [36-37]

	EVA resin		
	EVA-33	**EVA-28**	**EVA-18**
Trade Name	EVAFLEX	POLENE	POLENE
Grade	EV 150	MV 1055	N 8083
VA Content [%wt]	33	28	18
Manufacturer	DuPont-Mitsui Chemical Co.,Ltd. (Japan)	TPI Polene (Thailand)	TPI Polene (Thailand)
MFI [g/10min]	30	8	2.3
Tensile Strength [MPa]	8.8	27	24
Vicat Softening Temperaature [°C]	33	49	62

Table 3.2 Organic peroxides data [8]

Type	Chemical name	Trade name	Assay	Active Oxygen [%]	Half-life [°C] 10 hr.	1 hr.
Dialkyl peroxide	Dicumyl peroxide	***DCP***	39.5-41.5	2.34-2.46	117	137
Peroxyester peroxide	OO-t-Butyl O-(2-Ethylhexyl) monoperoxy-carbonate	***Lupersol TBEC***	≥95	≥6.2	100	121
Peroxyketal peroxide	1,1-Bis-(t-Butylperoxy) 3,3,5-trimethyl-cyclohexane	***Lupersol 231***	≥92	≥9.73	96	115

Table 3.3 Silane coupling agent data [5]

Chemical name	Trade name	Manufacturer
3-trimethoxysilylpropyl methacrylate	***DYNASYLAN MEMO***	JJ-Degussa Chemicals (Thailand)

Table 3.4 Other additives data [5]

Chemical name	Trade name	Manufacturer
Hindered Amine Light Stabilizer (HALS) Bis(2,2,6,6-tetramethyl-4-piperidinyl) sebacate	***Lowilite 77***	Great Lakes Chemical Corporation (USA)
Ultraviolet Light Absorber 2-Hydroxy-4-octoxybenzophenone	***Lowilite 22***	Great Lakes Chemical Corporation (USA)
Antioxidant Tris(Nonylphenyl)phosphate	***Naugard P***	Sigma-Aldrich (USA)

3.1 Mixing and compounding of EVA compounds

EVA resins were mixed with organic peroxides, silane coupling agent and other additives at room temperature. Those additives were dissolved in acetone 20 ml before sprayed over the EVA resins. Then they were compounded by twin-screw extruder (Plasti-Corder PL2100, OHG Duisburg) with L/D ratio equal to 16.7 (screw diameter 19.7 mm, die diameter 3 mm), screw speed 20 rpm at given barrels temperature 80°C and die temperature 85°C. Finally, the compounds were sheeted by two-roll mill at 40°C for 5 min. The compositions of EVA compounds can be divided into 3 groups:

1. EVA compounds for crosslinking characteristics test

The composition of EVA compounds was presented in Table 3.5.

Table 3.5 Composition of EVA compounds for crosslinking characteristics test [5]

Composition	Parts [phr]
EVA resin	100
Organic peroxide	1.50
UV absorber	0.30
UV stabilizer	0.10
Antioxidant	0.20
Silane coupling agent	0.25

2. EVA compounds for effect of organic peroxide concentrations test

The organic peroxides were varied as 0.10, 0.15 and 0.20 phr for each compound while other compositions were used as shown in Table 3.5.

3.2 Crosslinking characteristics measurement

The crosslinking characteristics were measured by a Monsanto Moving Die Rheometer (MDR 2000, Alpha Technologies) according to ASTM D 5289-97. About 4 g samples of the respective compounds were tested at temperature ranging from 150-170°C and measuring time 15 min. The torque measured data were collected as real time record. The crosslinking characteristics

were presented by torque-time cure curves. Cure time (t_C10 and t_C90) and cure rate index (CRI) were calculated following Eq. (2-12) and Eq. (2-14) respectively.

$$t_Cx \text{ is the time to produce torque } (\tau) = (x/100) \bullet (M_H - M_L) + M_L \quad (2\text{-}12)$$

$$\text{Cure Rate Index (CRI)} = 100 / (t_C90 - t_C10) \quad (2\text{-}14)$$

Where M_L = minimum torque [dNm]

M_H = maximum torque [dNm]

x = percent state of cure

t_Cx = time to a given percent (x) state of cure

3.3 Determination of activation energy using model-free method

The conversion at any given time can be calculated from the cure curves as follows Eq. (2-15)

$$\alpha_t = \frac{C_t}{C_\infty} \cong \frac{(\tau_t - M_L)}{(M_H - M_L)} \quad (2\text{-}15)$$

Where C_t = concentration of crosslinks at time t

C_∞ = final concentration of crosslinks ($t \rightarrow \infty$)

τ_t = torque at time t [dNm]

M_L = minimum torque [dNm]

M_H = maximum torque [dNm]

After applied Eq. (2-15), the conversion curves can be drawn. Then reaction times were calculated at conversion ranging from 0.1-0.9 by interpolation. Model-free method was used to calculate activation energy at progressive degrees of conversion without any modelistic assumptions. The standard model-free method was presented in Eq. (2-21).

$$-\ln t_\alpha = \ln\left(\frac{A}{g(\alpha)}\right) - \frac{E_{a,eff}}{RT} \quad (2\text{-}21)$$

A plot of –ln t_α versus $1/T$ at each α yields $E_{\alpha,eff}$(from the slope) for that α regardless of the model.

3.4 Gel content measurement

After test the crosslinking characteristics, the cured samples were cut and weighed approximate 1.4-1.5 g. Then put it in 100 ml of xylene at give temperature 110°C, and immersed to stand for 12 hours. After extraction, the undissolved samples were collected by a 30-mesh wire cage and dried at 110°C for 8 hours under vacuum. Finally, reweighed the after dried product and calculated their gel contents using Eq. (2-23).

$$\text{Gel Content}[\%] = \left(\frac{\text{weight of undissolved content}}{\text{original weight of sample}} \right) \times 100 \qquad (2\text{-}23)$$

3.5 Light transmission measurement

The samples for light transmission measurements were prepared by hot compression machine (Compress machine LP20, Lab Tech Engineering Co., Ltd.). The Teflon mold size was 5" x 5" and Teflon spacer was 0.5 mm thick. The compression was pre-pressed at give temperature 85°C for 3 min. and then operated at give temperature 150°C for 15 min and cooled with cool water for 3 min.

The compressed sheets were cut to small rectangular shape and put in paper frames. The Light transmission was measured by UV-Vis spectrophotometer. Firstly, turned on the instrument and selected 'Transmittance Mode' with scanning wavelength 550 nm. Secondly, scanned blank for setting base line. Then put sample into the sample holder. Finally, scanned the samples and changed to 'Statics Mode' for data output.

Chapter 4

Results and Discussion

Crosslinking reactions by using organic peroxides and silane coupling agent are essential phenomena during the lamination-curing process. Therefore, to understand cure characteristic is an important key point to improve the quality of encapsulating materials. The isothermal real-time torque measurement by using MDR instrument is comfortable and reliable to investigate the cure characteristic of EVA-based encapsulant for PV modules. This research studied the effect of organic peroxides on crosslinking characteristics of EVA-based encapsulants which contained 18, 28 and 33 %wt VA contents. The crosslinking reactions can be described by multi reaction mechanism which summarized in Chapter 2. Furthermore, the isothermal isoconversional (model-free) method was applied to isothermal kinetic analysis of these crosslinking reactions. In this chapter we examined the results of organic peroxides on EVA 33 %wt (EVA-33) which is a general commercial grade of PV encapsulant, and studied on the point of their kinetics, finally, developed the in-house EVA-based encapsulant using EVA 28 %wt (EVA-28) which is a domestic produced EVA grade.

4.1 Effect of VA contents on crosslinking characteristics

EVAs which contain 18, 28 and 33 %wt VA contents were compounded with dicumyl peroxide (DCP; Dialkyl peroxide class) and cured at given temperature 150°C for cure time 30 min. The cure curves are shown in Figure 4.1 (torque data of these compounds are tabulated in Appendix A-1). It can be seen that these compounds are cured with continuously increasing torque (i.e. marching trend). For EVA-33 compound, its torque remained constant around first 2 min that implied to the crosslinking reactions did not occur while molten EVA filled in the molds. Then the crosslinking reaction had began and dramatically increased until 5 min of cure time after that the compound was over-cure. EVA-28 and EVA-18 compounds produced cure curves similar to EVA-33 compound. The cure properties of these compounds are located in Appendix A-2. The maximum torque (M_H) decreases with increasing VA content. It is affected by their physical property, that is, high VA content compound is softer than low VA content compound. On the other hand, VA contents do not effect on optimum cure time. It can be seen that their optimum

cure time are similar. Therefore, the use of EVA-18 and EVA-28 instead of EVA-33 would be probably possible.

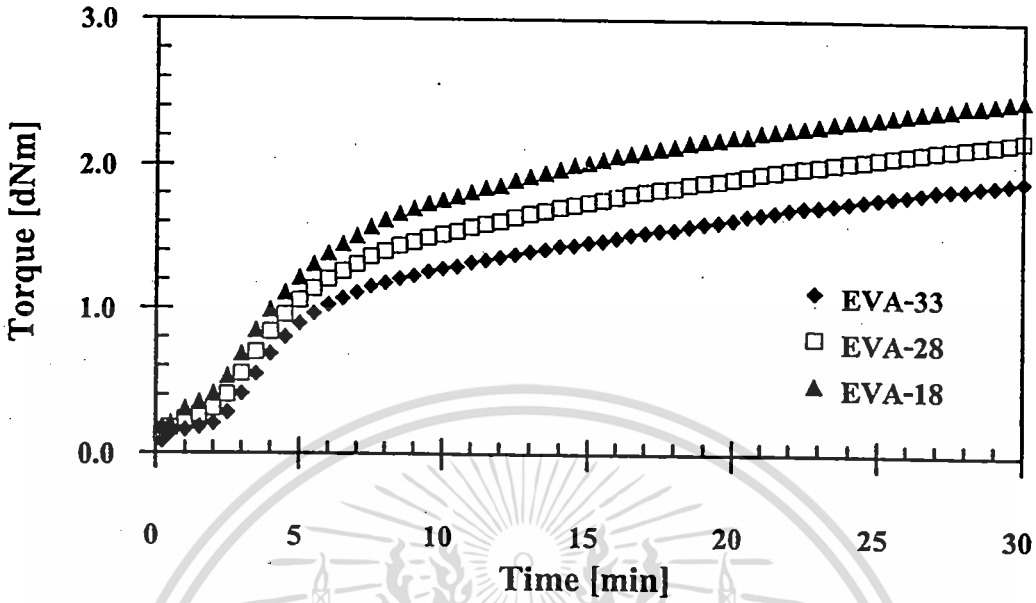

Figure 4.1 Effect of VA content on cure curves of EVAs/Dialkyl peroxide compounds at cure temperature 150°C.

4.2 Effect of organic peroxides on crosslinking characteristics

In order to investigate the effect of organic peroxides, the encapsulant samples were cured at constant temperature. As isothermal curing, the thermal decomposition of organic peroxides in encapsulant crosslinking reactions depends on their molecular structure, which has an important effect on the lamination-curing time. Three classes of organic peroxide candidates which are (1) dialkyl peroxide; (2) peroxyester peroxide; and (3) peroxyketal peroxide were used. Firstly, these candidates were compound with EVA-33 as formulated in Table 3.5. Then they were characterized their cure behavior by MDR. The torque-time cure curves as well as cure time and cure rate were determined.

4.2.1 Effect of dialkyl peroxide on crosslinking characteristics

Dicumyl peroxide (DCP) is white crystals peroxide. It is common peroxide for crosslinking applications. The thermal decomposition of DCP is demonstrated in Figure 4.2. As shown in the figure, DCP decomposes to two cumyl radicals and then these radicals can be reacted with hydrogen abstraction to produce hydroxyisopropylbenzene (cumyl alcohol) or

beta-scission reaction to produce methyl radicals and acetophenone as a by-product. These methyl radicals are high energy level of 439.1 kJ/mol. Peroxides which generate free radical ≥ 418.6 kJ/mol possess high crosslinking efficiency due to their ability to abstract secondary hydrogen commonly present in most crosslinkable polymers [9]. The DCP crosslinking mechanism is illustrated in Figure 2.7. The typical decomposition products are methane, acetophenone, and cumyl alcohol. The aromatic by-products or chromophores in the curing step are caused of discoloration of the cured EVA [4]. Discoloring of EVA can reduce PV module efficiency because of decreased light transmittance [5].

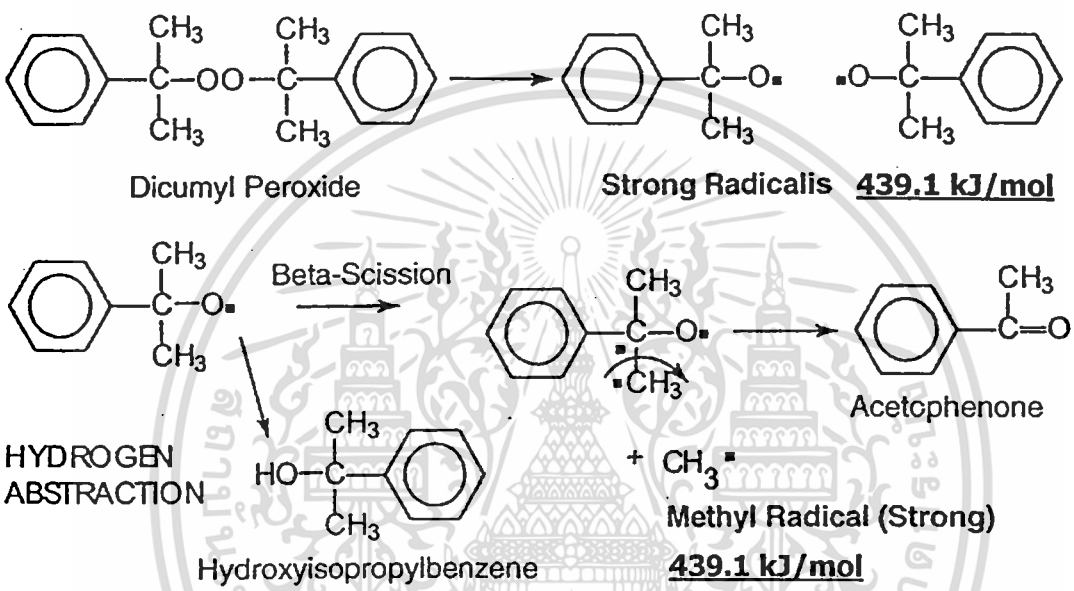

Figure 4.2 Thermal decomposition of DCP (Dialkyl peroxide class) [9].

The cure curves of EVA-33/Dialkyl peroxide compounds were presented in Figure 4.3. It shows that cure reaction of temperature 150°C and 160°C are not adequate as a marching trend. The plateau curve as shown on temperature 170°C is convinced for sufficient cure. Optimum cure time (t_c90) of these cure curves are 23.23, 19.55 and 7.03 minutes, respectively. Cure rate index (CRI) of 150°C and 160°C are quite low, on the contrary, CRI of 170°C cure curve is triple high value. The cure properties tables of these curves are located in Appendix A-1. For the purposing of productivity and cost reduction as well as high quality product, lamination-curing processing could be operated at lowest cure temperature and shortest cure time. Even though DCP can produce strong free radicals, its half-life temperature is significantly high. So that, it has to use long time to decompose at low temperature, or it must be heated up to higher temperature to produce free radicals for short cure time. Moreover, at high

cure temperature and/or long cure time can generate acetophenone which causes the yellowing EVA. It can be seen that DCP is not suitable peroxide for EVA-based encapsulant crosslinking because it has to use operating temperature up to 170°C to complete its crosslinking reactions and the final product has light yellow color.

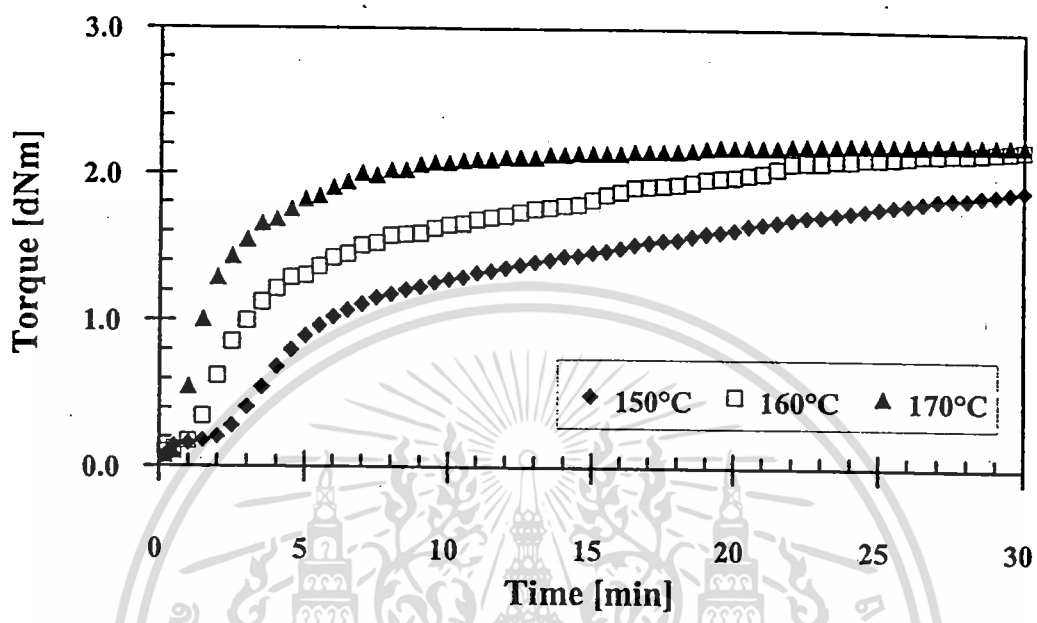

Figure 4.3 Effect of temperature on cure curves of EVA-33/Dialkyl peroxide compounds.

4.2.2 Effect of peroxyester peroxide on crosslinking characteristics

Lupersol TBEC™ is well-known peroxide for fast cure formulation as 15295P. It is pure liquid peroxyester peroxide. This peroxide provides good crosslinking efficiency, and has a high molecular weight of 246 g/mol. The suggested temperature range of this peroxide usage is ~145 to 180°C for the complete cures in 2 hours to about 5 minutes, respectively [9]. Furthermore, it is non-aromatic, non-discoloring, and does not produce decomposition by-products which would lead to bloom [8]. Figure 4.4 is shown the thermal decomposition of Lupersol TBEC. It can generate high energy radicals of 439.5 kJ/mol. These radical are less stable, strong radical which would be easily crosslink.

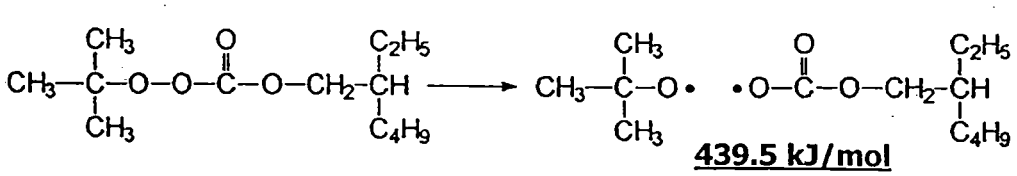

Figure 4.4 Thermal decomposition of Lupersol TBEC™ (Peroxyester peroxide class) [9].

Cure curves of EVA-33/Peroxyester peroxide compounds at temperature 150°C, 155°C and 160°C are exhibited in Figure 4.5. As usual, these cure curves significantly increase up to about 5 minutes and gradually attain the plateau curve. As well as, maximum torque increased with cure temperature increased. These compounds show that this formulation can be used for crosslinking in this temperature range. Optimum cure time (t_c90) of these curves are 7.93, 6.63 and 4.52 minutes, as well as the CRI are 14.37, 16.85 and 25.74 min^{-1} respectively. These results are similar to other reports for 15295P (fast cure formulation) [33-35]. Lupersol TBEC has low half-life temperature (1 hr half-life at 121°C). This half-life temperature is considerable effect on cure performance. Czanderna and Pern [4] recommended the 15295P formulation to PV industry because the A9918P (standard cure formulation which used Lupersol 101, dialkyl peroxide, as curative) degraded faster than the 15295P under identical accelerated test conditions. Furthermore, they studied the effect of cure temperature and cure time and found that the standard-cure A9918P increased the concentration of the chromophores as the cure temperature was increased from 130°C to 175°C for a fixed cure tine of 30 minutes, but the fast-cure Lupersol TBEC produced almost no net increase in the chromophores in the same temperature range for cure time of 15 minutes. In addition, shorter cure time could reduce concentration of UV-excitable chromophores that might significantly influence the photothermal stability of EVA [32].

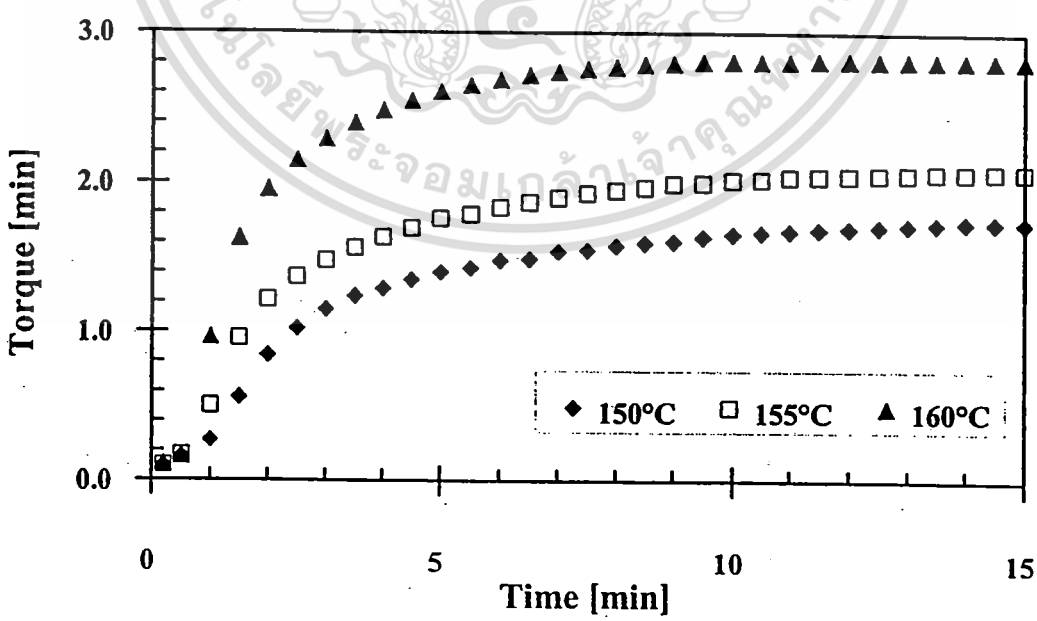

Figure 4.5 Effect of temperature on cure curves of EVA-33/Peroxyester peroxide compounds.

4.2.3 Effect of peroxyketal peroxide on crosslinking characteristics

The last candidate of peroxide crosslinking systems is peroxyketal peroxide. The peroxyketal peroxide generates a mixture of weak and high energy free radicals as shown in Figure 4.6. The mechanism of decomposition of peroxyketal peroxides are complex and may vary with specific structures. This research used Lupersol 231 (1 hr half-life at 115°C) for modified formulation. Because this peroxide has lowest half-life temperature and can produce 2 strong radicals and 1 weak radical. Thus, it would be a better choice than peroxyester peroxide for decreasing lamination-curing time. Moreover, the typical decomposition products such as methane, acetone, t-butyl alcohol, CO_2 and other products are non-discoloring [8-9].

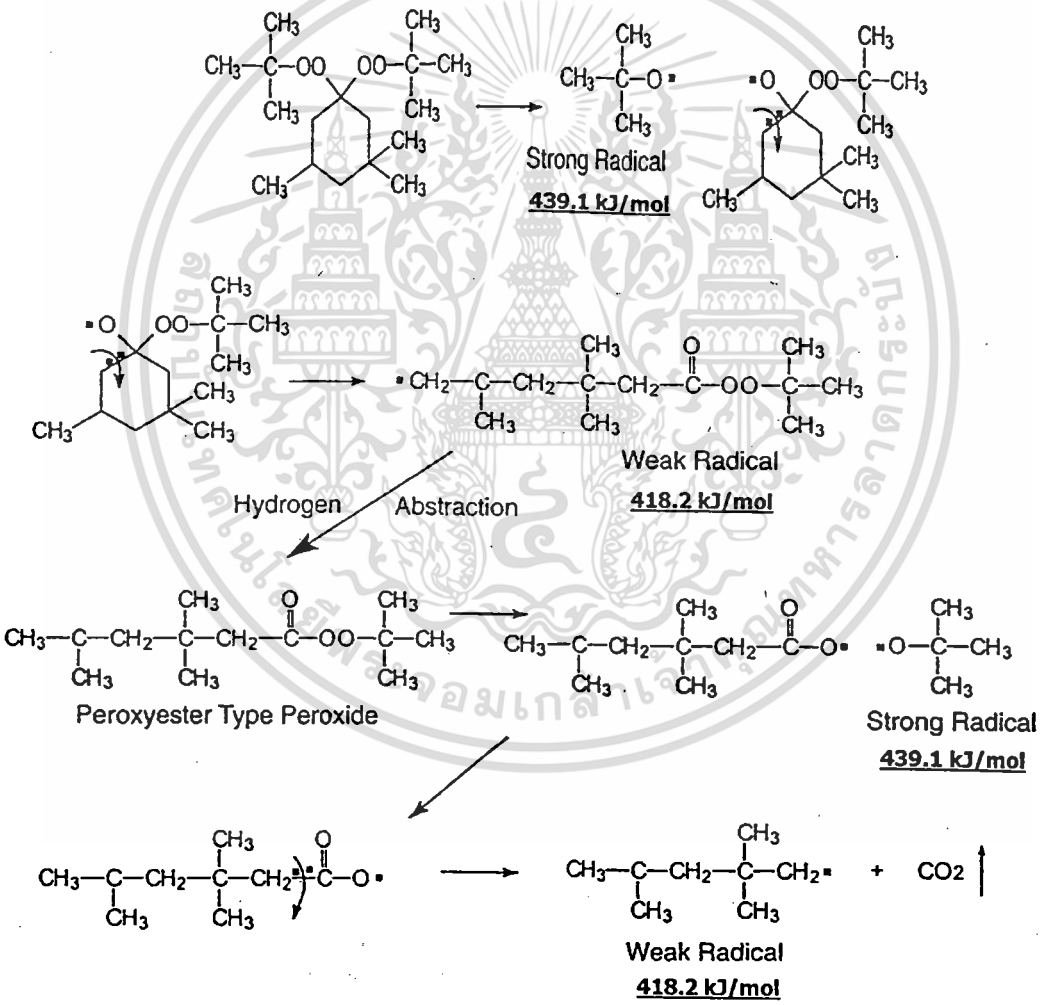

Figure 4.6 Thermal decomposition of Lupersol 231 (Peroxyketal peroxide class) [9].

Figure 4.7 shows that cure curves of EVA-33/Peroxyketal peroxide compounds at given temperature 150°C, 155°C and 160°C for 15 minutes. It can be seen that torque dramatically increased and reached the equilibrium state of cure within cure time 3 minutes. While increasing of cure temperature did not significantly effect on maximum torque. Optimum cure times (t_c90) of these compounds are 3.15, 2.29 and 1.30 minutes for cure temperature 150°C, 155°C and 160°C, respectively. Because of the peroxyketal peroxide has low half-life temperature and also can produce both strong and weak free radicals it would be an extreme active for crosslinking reactions.

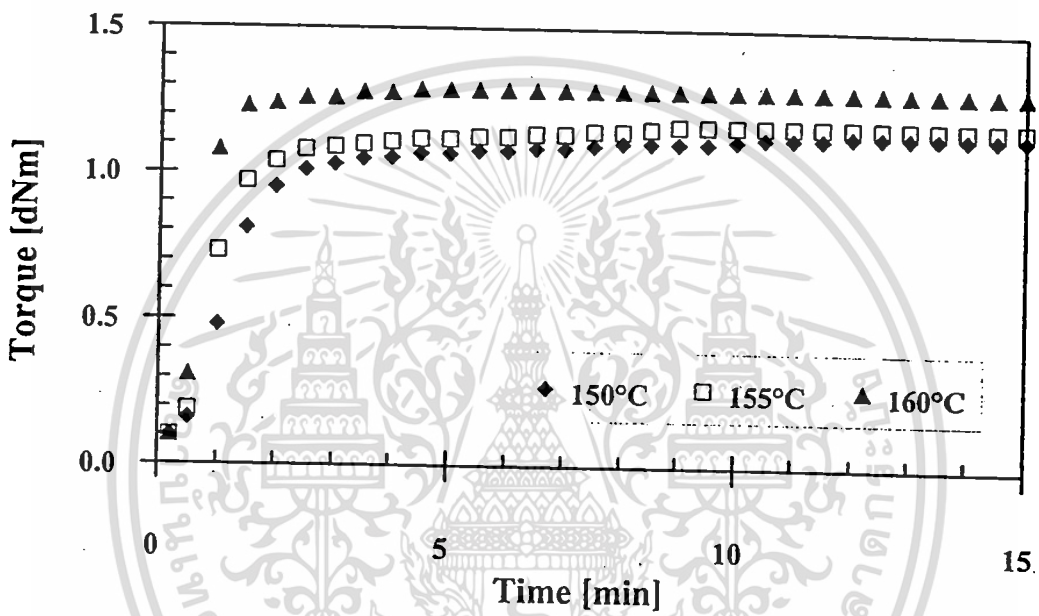

Figure 4.7 Effect of temperature on cure curves of EVA-33/Peroxyketal peroxide compounds

4.2.4 Comparison of crosslinking characteristics with organic peroxides

Crosslinking characteristics of EVA-33/Peroxides compounds including cure curve, torque difference, cure time and cure rate index are summarized in this section. Cure curves of 3 EVA-33/Peroxides compounds compared with the 15295P (commercial encapsulant film) at given cure temperature 150°C and cure time 15 minutes are presented in Figure 4.8. It can be seen that torque of EVA-33/Dialkyl peroxide compound slowest developed, on the contrary, EVA-33/Peroxyketal peroxide compound can be cured fastest and completely. The peroxyketal peroxide can quickly decompose and generates free radicals and then reacts during crosslinking reactions that obviously indicate on its cure curve. EVA-33/Peroxyester peroxide is a bit different from the 15295P, that is, this compound was cured faster than the

15295P. It could be an effect of other additives which used in the formulation. Dick [9] found that other additives could have a dramatic effect on peroxide cures. From these cure curves we can conclude that peroxyketal peroxide has efficient performance for EVA-based encapsulant.

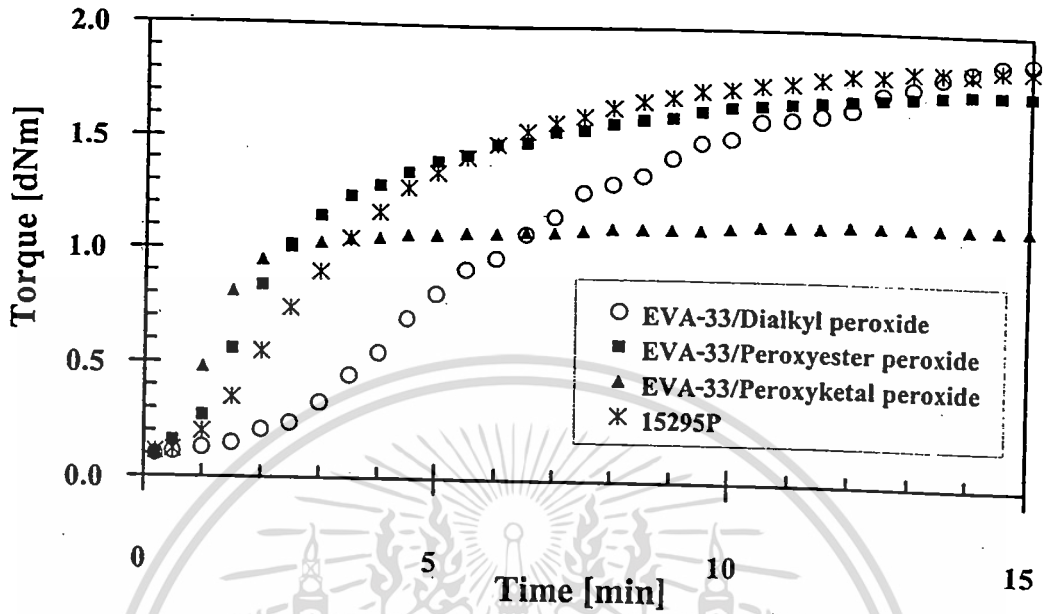

Figure 4.8 Effect of organic peroxide on cure curves of EVA-33/Peroxides compounds at cure temperature 150°C.

In addition to the experimental results from MDR, the torque difference between maximum and minimum torque (M_H-M_L) which directly related to crosslinking density is shown in Figure 4.9. It can be seen that torque difference increases with increasing temperature for all types of peroxides. As shown in cure curves above, rising cure temperature leads peroxides faster decompose themselves to free be radicals and then crosslinking reactions can also occur spontaneously. Hence, the torque of high cure temperature is generated rapidly which depends on their half-life temperature. Besides, the torque difference of EVA-33/Peroxyester peroxide compound quite more extends with cure temperature than other compounds.

Cure time at 90% of cure state (t_c90) of these compounds are compared in Figure 4.10. It shows that cure time decreases with increasing temperature. EVA-33/Dialkyl peroxide has slow cure time up to 20 minutes for 150 and 160°C and then dramatically decreases 3 times to 7 minutes on curing temperature 170°C. EVA-33/Peroxyester peroxide and EVA-33/Peroxyketal peroxide compounds have obviously fast cure time. It revealed that peroxyketal peroxide can be cured faster than peroxyester peroxide about 2.5 times at cure temperature 150°C and about 4 times by increasing cure temperature 10°C. Thus it would be possible to use

peroxyketal peroxide at lower cure temperature than 150°C in order to avoid any thermal degradation occur while the present commercial encapsulant can not attain the same cure level. It is emphasized in Figure 4.11 that displays the cure rate index (CRI) of these compounds. In addition, the efficiency of dialkyl peroxide at 170°C is approximately equal to peroxyester peroxide at 150°C.

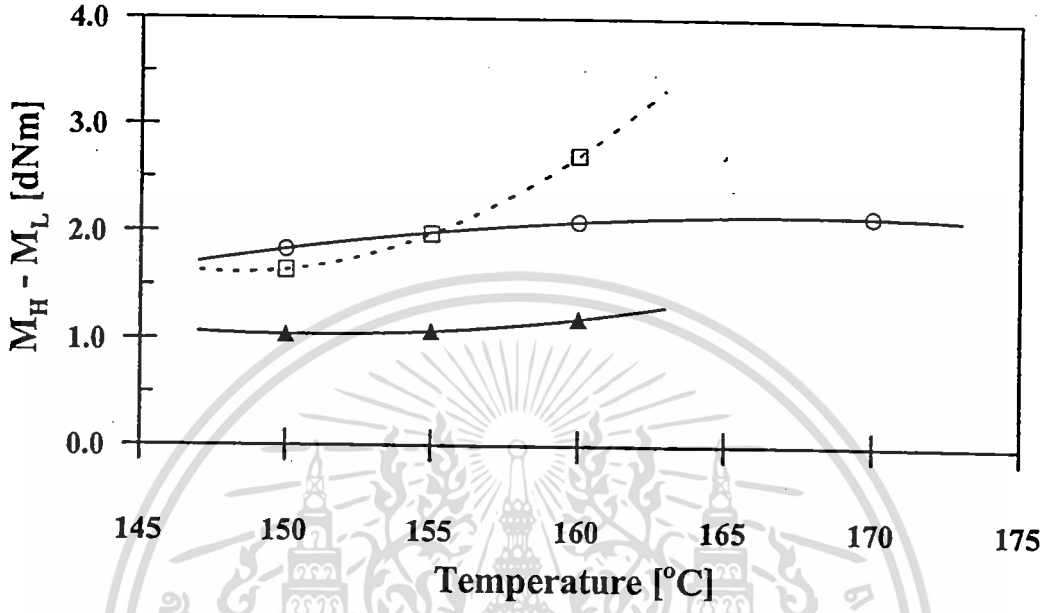

Figure 4.9 Effect of temperature on torque difference ($M_H - M_L$) of EVA-33/Peroxides compounds. (●) EVA-33/Dialkyl peroxide; (□) EVA-33/Peroxyester peroxide; (▲) EVA-33/Peroxyketal peroxide.

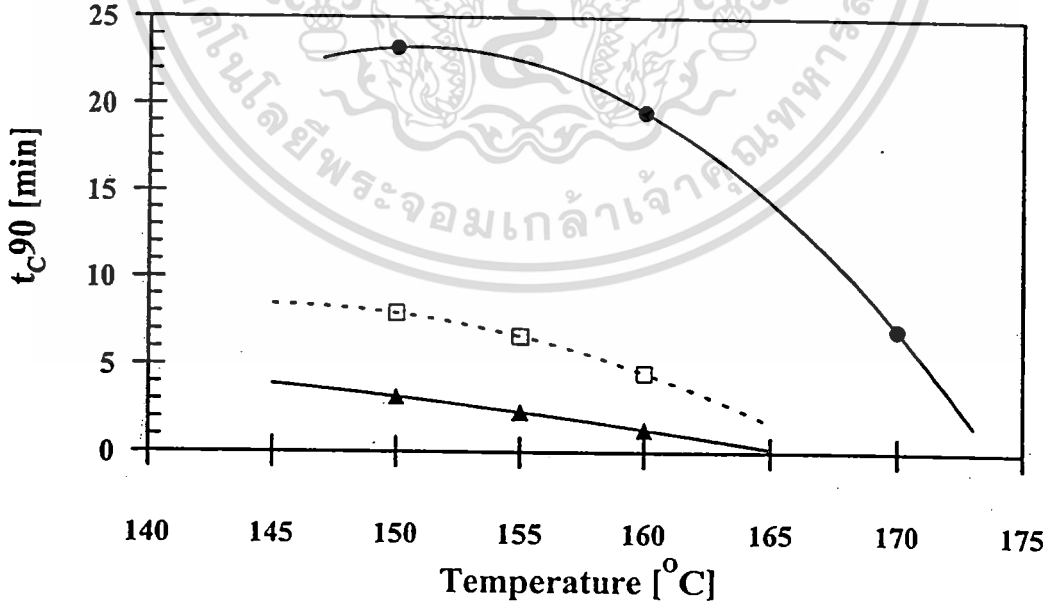

Figure 4.10 Effect of temperature on t_C90 of EVA-33/Peroxides compounds.

(●) EVA-33/Dialkyl peroxide; (□) EVA-33/Peroxyester peroxide;

(▲) EVA-33/Peroxyketal peroxide.

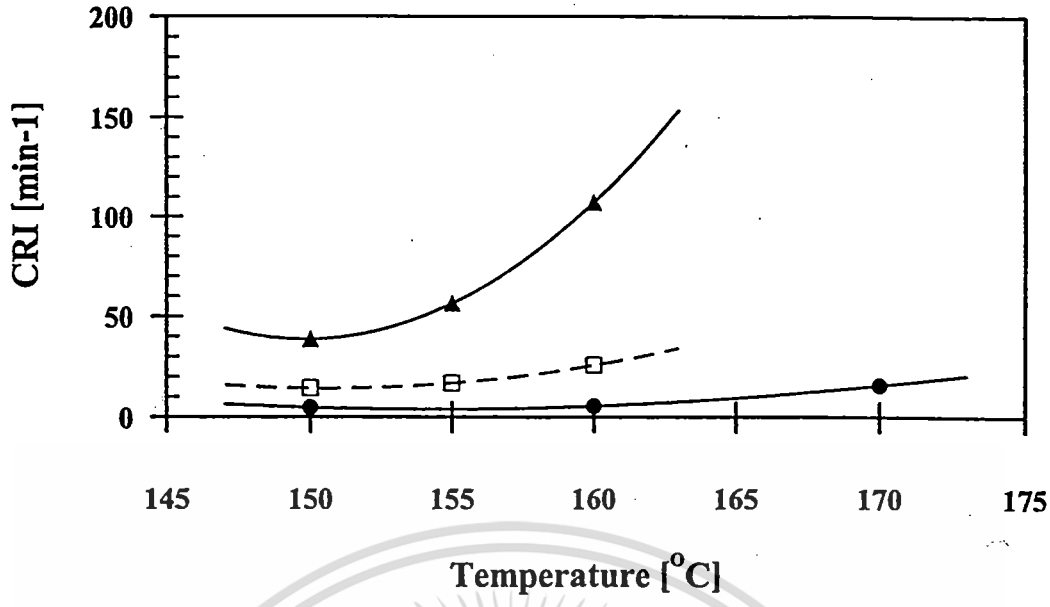

Figure 4.11 Effect of temperature on cure rate index (CRI) of EVA-33/Peroxides compounds.
(●) EVA-33/Dialkyl peroxide; (□) EVA-33/Peroxyester peroxide;
(▲) EVA-33/Peroxyketal peroxide.

Nevertheless, in lamination-curing process by using vacuum laminator, it can be divided into 2 processes; lamination and curing. Specific processing conditions, i.e., temperature, time, and pressure are not readily known because they are considered proprietary information by PV manufacturers [38]. In general, solar cell and other assembly parts as shown in Figure 1.1 were put into the laminator chamber. Then the lamination process was operated, EVA was melt and spread cover solar cells and bonded itself to cover glass and backing materials. The lamination temperature is generally not over 120°C. In this step, thermal decomposition of organic peroxide must be avoided because the peroxide such as Lupersol TBEC has a tendency to generate bubbles from CO_2 and other gaseous organics. Moreover, prior industry experience emphasized that higher lamination temperatures were unfeasible at temperature approaching 155°C. Thus, the temperature controlling and thermal decomposition of organic peroxide information are necessary required for PV manufacturers to prevent bubble formation. In curing process, temperature was increased up to 150 °C to 160°C (general curing temperature) and the crosslinking reactions could be accomplished in 7 minutes at 150°C (for 15295P).

Wohlgemuth and Shea [34] reported that curing temperature had influence on peroxide decomposition products from the IR analysis of the thermal effluents from EVA encapsulants. That analysis concluded that water evolved at 105°C, CO_2 at 120°C, acetone and

t-butanol at 177°C and acetic acid at 205°C. It was further determined that at least 1.5 %wt water could be present in a 33%wt VA containing EVA following short exposure to air. They suggested that completely dried EVA encapsulants under vacuum for 18 hours at 50°C had no bubbles formation during lamination process.

Therefore, the use of peroxyketal peroxide as curative in EVA-based encapsulant formulation is an interesting and possible choice for the new formulation. This peroxide has low half-life temperature and non-discoloring by-products. EVA/Peroxyketal peroxide formulation can be produced by film extrusion and pre-dried before using in lamination process. This film would be used under low cure temperature and time conditions. The combination of these factors could be prevent bubble formation and obtain good yield of crosslinked EVA.

4.3 Effect of organic peroxide concentrations on crosslinking characteristics

Typically peroxide concentrations range from 0.5 to 2.0 parts by weight per one hundred parts of resin (phr) is recommended [8]. At lower concentrations, curing process may be slow and physical property deterioration may be encountered. Higher peroxide concentrations are not cost effective since initiator is lost in wasteful side reactions. Thus this work the effect of peroxide concentration ranging from 0.10 to 0.2 phr was determined.

EVA-33/Peroxyester peroxide compounds were cured at cure temperature 150°C for cure time 15 min as shown in Figure 4.12. On the start of cure occurred, there are not different on their cure curves. After cure time 1 minute, it can be seen that torques of 0.10 and 0.15 phr increase and attain the optimum cure; moreover, the concentration 0.10 phr can be cured faster than the concentration 0.15 phr. The result is obviously determined that 0.10 phr has lower free radicals for initiating the crosslinking reactions. On the other hand, at concentration 0.20 phr, it shows the marching trend with the MH higher than other. It revealed that this concentration can generate excess of free radicals then crosslinking reaction can occur much more that other concentrations; the 15 minutes cure time may be not efficient to reach the optimum cure. Optimum cure times (t_c90) of these cures are 7.20, 7.93 and 8.73 minutes respectively. The CRI decreases with increasing peroxide concentration.

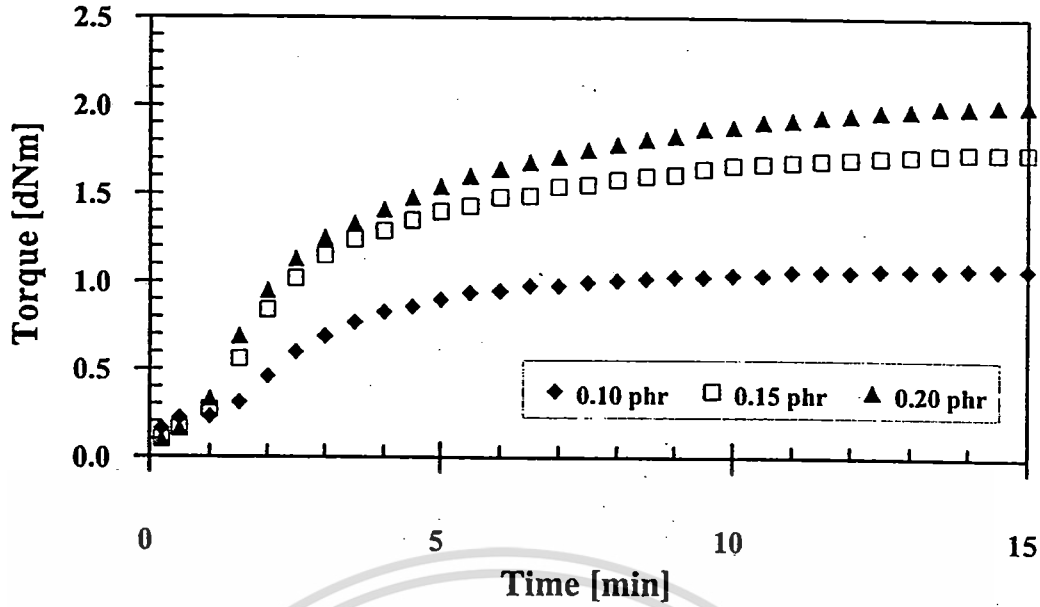

Figure 4.12 Effect of peroxide concentration on cure curves of EVA-33/Peroxyester peroxide compounds at cure temperature 150°C.

Figure 4.13 shows cure curves of EVA-33/Peroxyketal peroxide (0.10, 0.15 and 0.20 phr) compounds at cure temperature 150°C for cure time 15 minutes. It is quite similar to EVA-33/Peroxyketal peroxide compounds. All concentration compounds can be completely cured. Optimum cure time (t_c90) of 0.10 and 0.15 phr cure curves are 3.05 and 3.15 minutes but at 0.20 phr is up to 4.28 minutes. The CRI of the 0.20 phr is lower than the 0.10 and 0.15 phr approximately 33%.

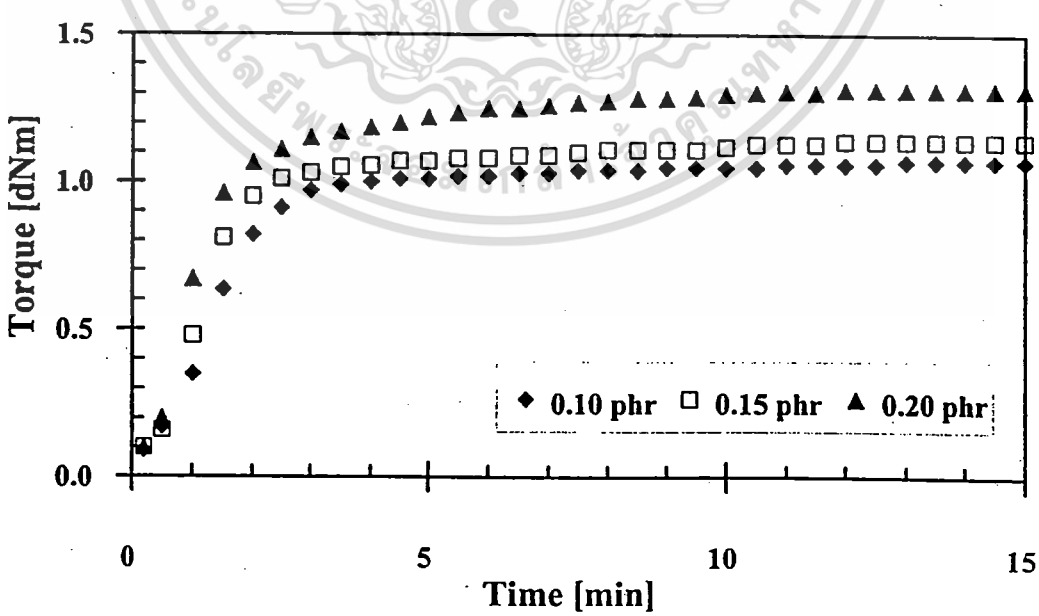

Figure 4.13 Effect of peroxide concentration on cure curves of EVA-33/Peroxyketal peroxide compounds at cure temperature 150°C.

4.4 Crosslinking characteristics of the in-house EVA formulations

EVA which contains 28 %wt VA content is a domestic produced resin. In order to investigate the possibility to replace imported EVA-33 by using EVA-28, it was formulated as EVA-33/Peroxides compounds. It was compounded with organic peroxides as EVA-28/Peroxyester peroxide compound and EVA-28/Peroxyketal peroxide compound. Crosslinking studies of these compounds were conducted at cure temperature 150°C, 155°C and 160°C at given cure time 15 minutes. The experimentally measured torque data as well as the cure curves and cure properties of these compounds are located in Appendix A-3 and A-4. The EVA-28/Peroxides compounds had shown similar trend of cure characteristics as EVA-33/Peroxides compounds. Figure 4.14 shows the comparison of cure curves of EVA-28/Peroxides and EVA-33/Peroxides compounds. It can be seen that the EVA-28/Peroxides compounds can be cured and attain the optimum cures.

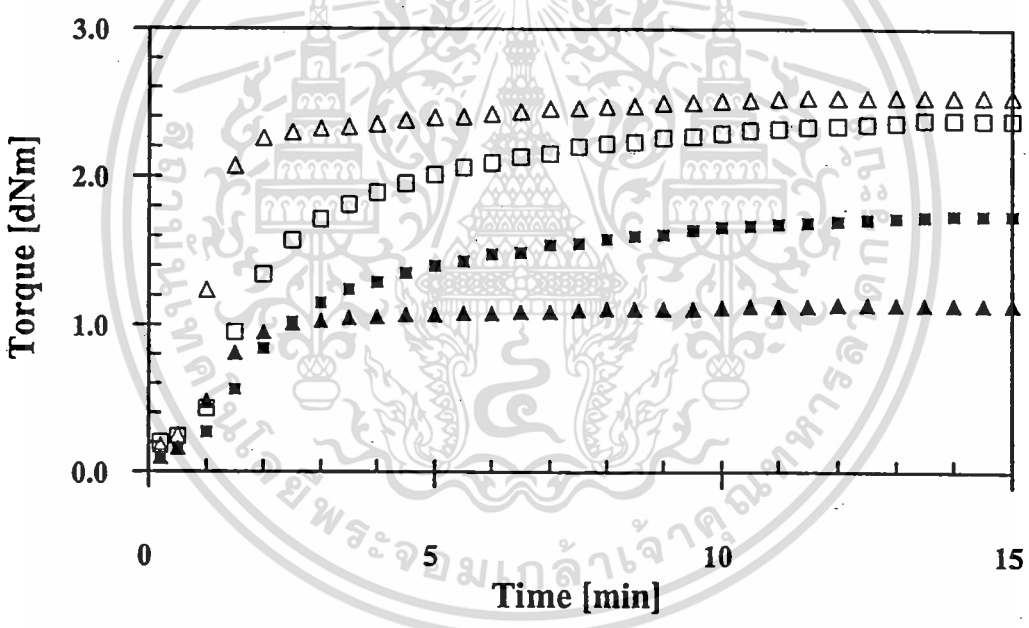

Figure 4.14 Cure curves of in-house EVA formulations compared with EVA-33 compounds at cure temperature150°C.

(■) EVA-33/Peroxyester peroxide; (□) EVA-28/Peroxyester peroxide;

(▲) EVA-33/Peroxyketal peroxide; (△) EVA-28/Peroxyketal peroxide.

Moreover, the EVA-28 produces higher torque than the EVA-33 because amorphous phase of EVA-28 is less than EVA-33 [36-37]. The torque difference between maximum and minimum torque (M_H-M_L) of these compounds are shown in Figure 4.15. The torque differences increase with increasing temperature and the EVA-28/Peroxides compounds have higher to

torque difference than the EVA-33/Peroxides compounds at any temperatures. Furthermore, it can be seen that EVAs compounded with peroxyester have more strength than EVAs compounded with peroxyketal. Optimum cure time (t_c90) and CRI of these cures are presented in Figure 4.16 and 4.17, respectively. The optimum cure time and the CRI of EVA-28 and EVA-33 compounds are slightly different.

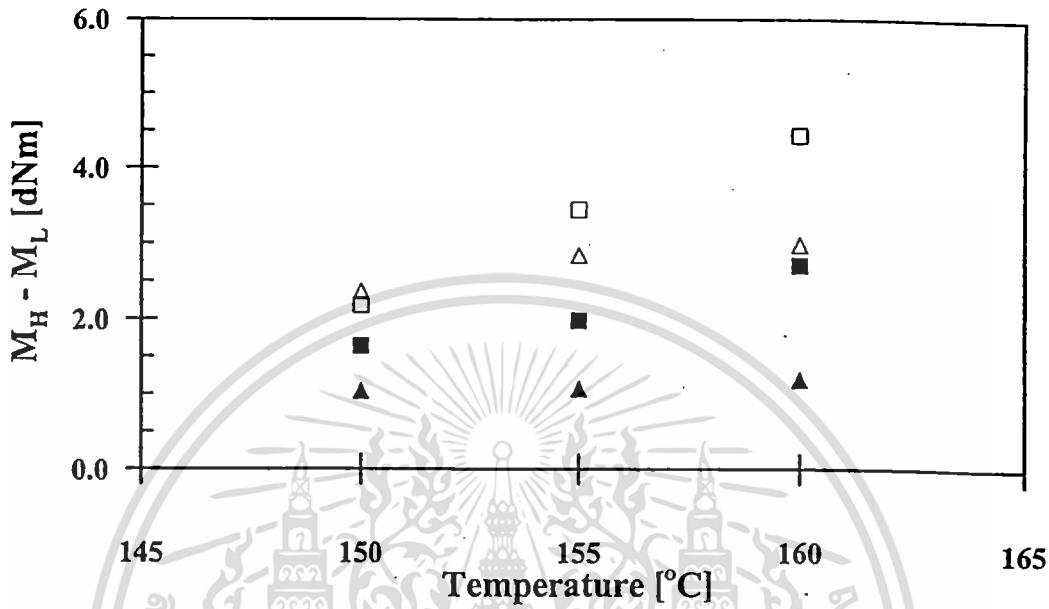

Figure 4.15 Effect of temperature on torque difference ($M_H - M_L$) of in-house EVA formulations compared with EVA-33 compounds for cure time 15 min.
(■) EVA-33/Peroxyester peroxide; (□) EVA-28/Peroxyester peoxide;
(▲) EVA-33/Peroxyketal peroxide; (△) EVA-28/Peroxyketal peroxide.

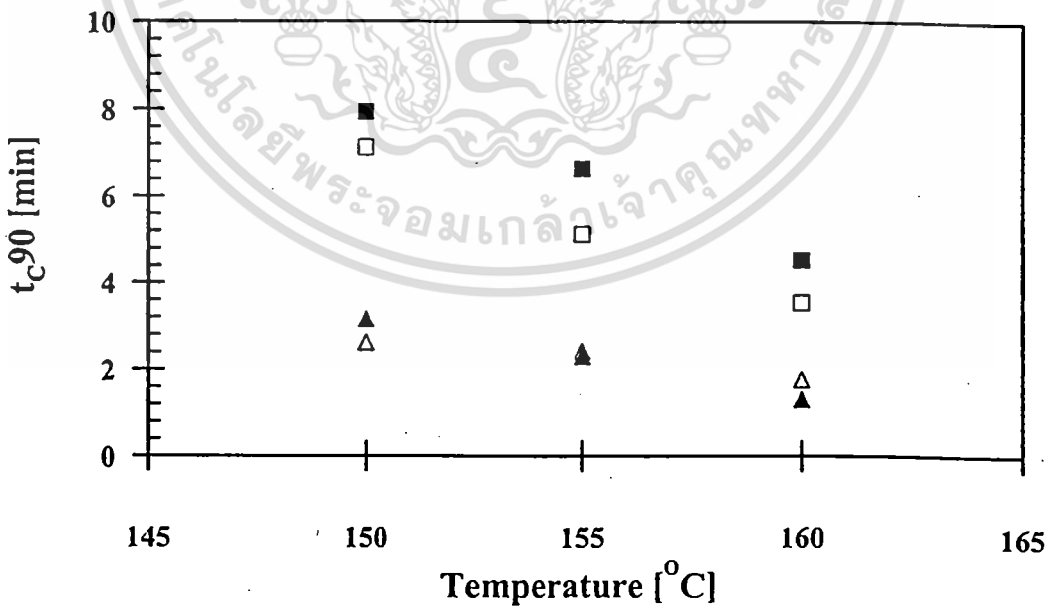

Figure 4.16 Effect of temperature on t_c90 of in-house EVA formulations compared with EVA-33 compounds for cure time 15 min.
(■) EVA-33/Peroxyester peroxide; (□) EVA-28/Peroxyester peroxide;
(▲) EVA-33/Peroxyketal peroxide; (△) EVA-28/Peroxyketal peroxide.

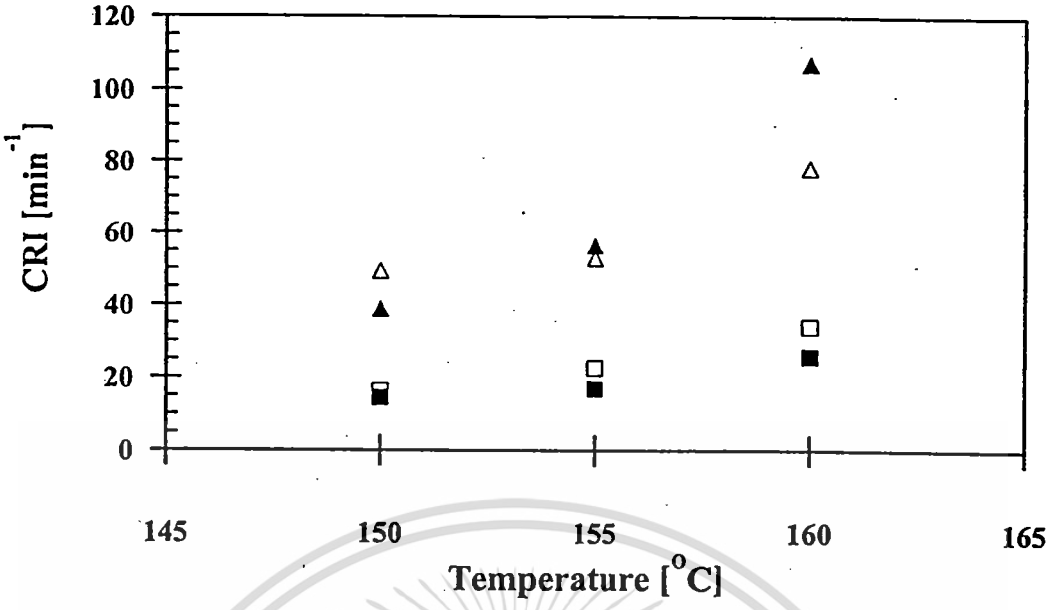

Figure 4.17 Effect of temperature on cure rate index (CRI) of in-house EVA formulations compared with EVA-33 compounds for cure time 15 min.
(■) EVA-33/Peroxyester peroxide; (□) EVA-28/Peroxyester peroxide;
(▲) EVA-33/Peroxyketal peroxide; (△) EVA-28/Peroxyketal peroxide.

The effect of peroxide concentrations in EVA-28 compounds was also studied. The peroxide concentration 0.10, 0.15 and 0.20 phr were compounded with EVA-28 and tested as EVA-33/Peroxides compounds. Cure curves and cure properties of these compound at these cure temperatures are located in Appendix A-2. Cure curves of the EVA-28 compounds show similar trend. The torque difference between maximum and minimum torque (M_H-M_L), optimum cure time (t_c90) and CRI of these compounds are shown in Figure 4.18 to 4.20, respectively. The torque differences of the EVA-28/Peroxides compounds are slightly different but significantly greater than the EVA-33 compounds. In addition, the torque difference of the EVA-28/Peoxides of peroxide concentration 0.10 phr is equivalent to the EVA-33/Peroxyester peroxide compounded with peroxide concentration 0.15 phr. It seems that we can reduce the peroxide amount in formulation approximately 33% when using EVA-28 resin. The optimum cure time of the EVA-28/Peroxides compounds are moderately lower than the EVA-33/Peroxides compounds at any peroxide concentrations. Because the EVA-28 has lower VA content than the EVA-33, that is, the crosslinking reactions can take place between the EVA-28 chains easily. Likewise, the CRI of the EVA-28/Peroxides are greater than the EVA-33/Peroxides compounds, especially, the CRI of the EVA-28/ 0.10 phr Peroxyketal peroxide compound is dramatically high.

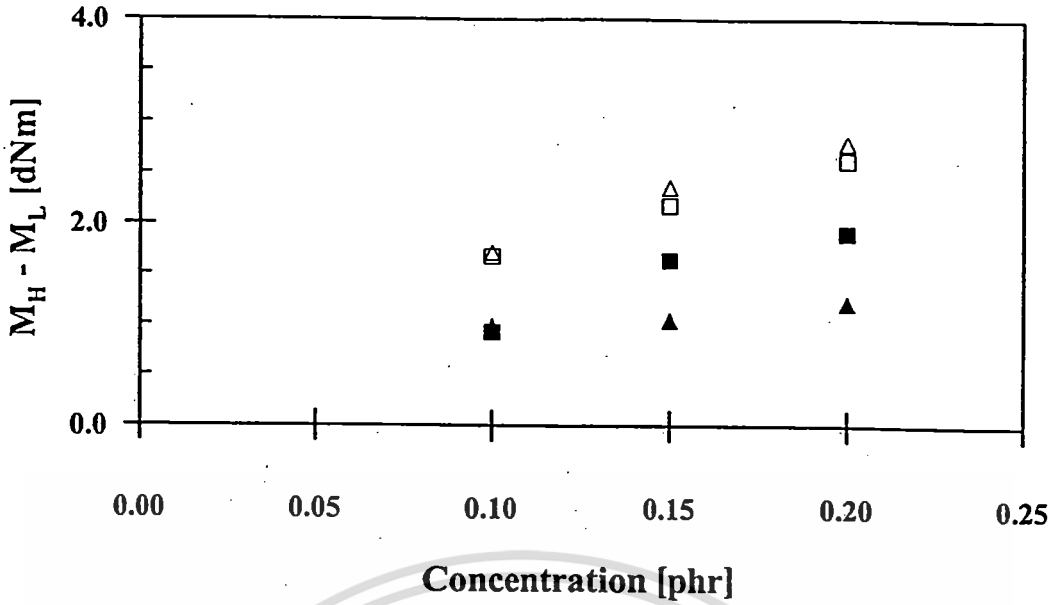

Figure 4.18 Effect of peroxide concentration on torque difference ($M_H - M_L$) of in-house EVA formulations compared with EVA-33 compoundsat cure temperature 150°C for cure time 15 min.
(■) EVA-33/Peroxyester peroxide; (□) EVA-28/Peroxyester peroxide;
(▲) EVA-33/Peroxyketal peroxide; (△) EVA-28/Peroxyketal peroxide.

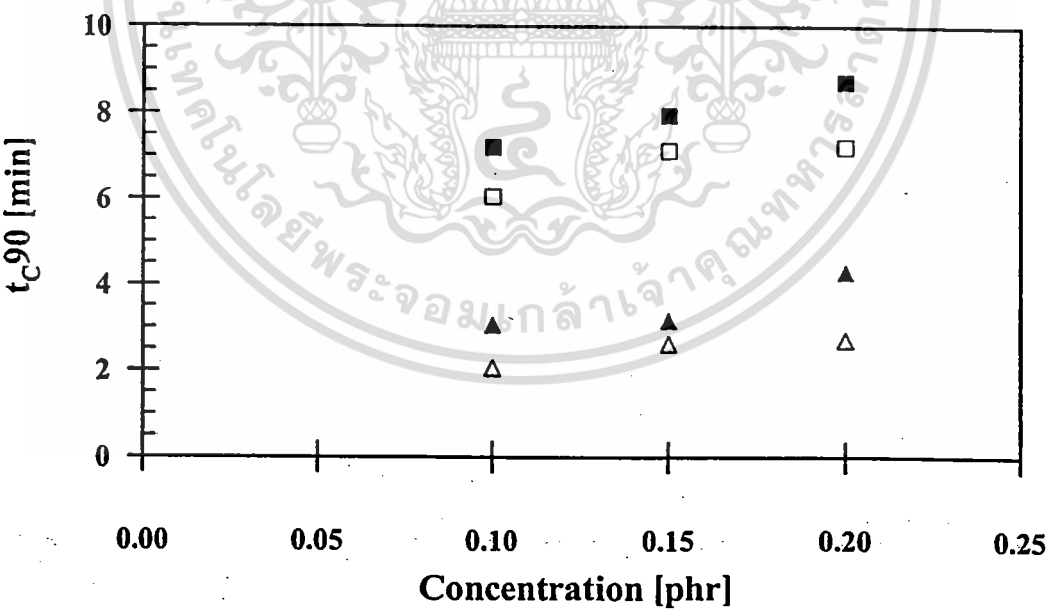

Figure 4.19 Effect of peroxide concentration on t_C90 of in-house EVA formulations compared with EVA-33 compounds at cure temperature 150°C for cure time 15 min.
(■) EVA-33/Peroxyester peroxide; (□) EVA-28/Peroxyester peroxide;
(▲) EVA-33/Peroxyketal peroxide; (△) EVA-28/Peroxyketal peroxide.

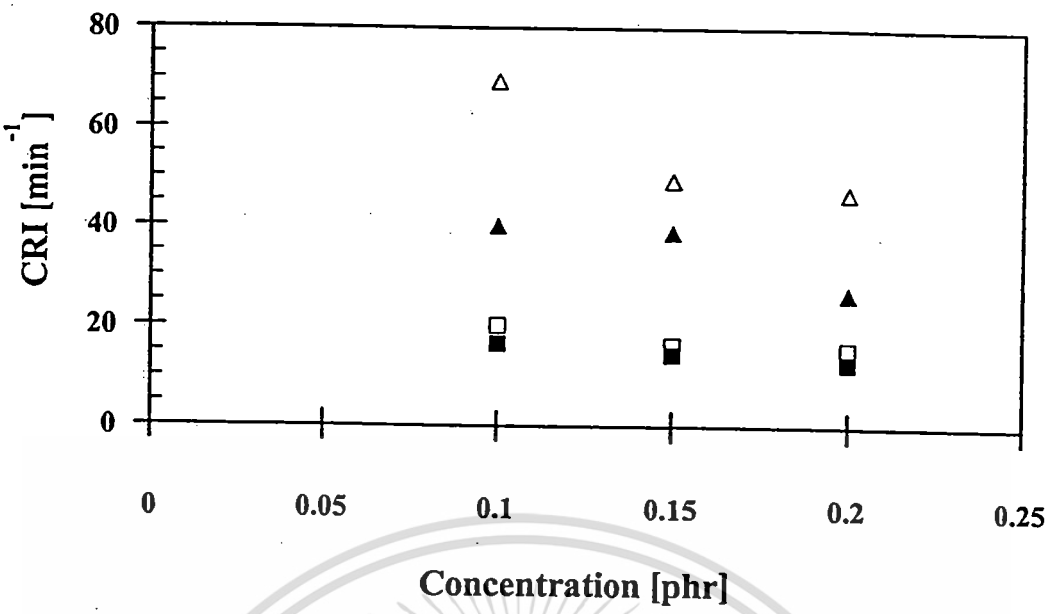

Figure 4.20 Effect of peroxide concentration on cure rate index (CRI) of in-house EVA formulations compared with EVA-33 compounds at cure temperature 150°C for cure time 15 min.
(■) EVA-33/Peroxyester peroxide; (□) EVA-28/Peroxyester peroxide;
(▲) EVA-33/Peroxyketal peroxide; (△) EVA-28/Peroxyketal peroxide.

As aforementioned it would be possible to use the domestic EVA resin which contains 28 %wt VA content. It can be seen that the EVA-28/Peroxides compounds have the ability to optimize cure as shown in their cure properties. Furthermore, the EVA-28 compounded with 0.10 phr of peroxyketal peroxide has considerably good performance for the encapsulant formulation.

4.5 Estimation of activation energy of crosslinking reactions

Solid-state kinetics was developed from reaction kinetics in homogeneous system (i.e. gases and liquids). The Arrhenius equation relates the rate constant of a simple one-step reaction to the temperature through the activation energy and pre-exponential factor. It has been generally assumed that activation energy and frequency factor remain constant, however, it has been shown [18-20] that in solid-state reactions these kinetic parameters may vary with the progress of the reaction. This variation can be detected by isoconversional methods. While this variation appears to be in conflict with basic chemical kinetic principles, in reality, it may not be. Such behavior may show that solid-state kinetics is more complex and/or multi-step compared to reactions in

homogeneous phases. Khawam et al. [18] noted that a variation in activation energy could be observed for both elementary and complex reactions. An elementary reaction could show variable activation energy during its progress due to the heterogeneous nature of the solid sample, which could cause a systematic change in reaction kinetics due to product formation, crystal defect formation, intra-crystalline strain or other similar effects. Solid-state reactivity of an elementary reaction could also be affected by experimental variables that could change the reaction kinetics by affecting heat or mass transfer at a reaction interface. If two or more elementary steps, each having a unique activation energy, control the rate of product formation, the reaction is usually called a complex reaction. In such a reaction, a change in the activation energy as the reaction progresses would be observed. This change will depend on the contribution of each elementary step, which gives an 'effective' activation energy that varies with reaction progress. Kinetic complexities are not limited to multiple chemical steps. They may also include physical processes (e.g. sublimation, localized melting, adsorption-desorption, diffusion of a gaseous product, particle size and morphology effects, etc.) that have different activation energies. Vyazovkin [39] defined term 'effective activation energy' as a parameter measured from a temperature dependence of the overall reaction rate. Sbrirrazzuoli and Vyazovkin [40] stated that if the changes in the mechanism are associated with changes in the activation energy, they can be detected by using the model-free isoconversional methods. These methods are based on the isoconversional principle that states that the reaction rate at constant extent of conversion is only a function of the temperature. The use of the model-free approach is recommended as a trustworthy way of obtaining reliable and consistent kinetic information from both isothermal and nonisothermal data.

As aforementioned the isoconversional model-free method was applied to determine the kinetics of EVA-33/Peroxides crosslinking reactions and compared with the model-fitting method by computer programmed calculation. The determination of activation energy of EVA/Peroxides crosslinking reactions had begun by the conversion calculation using Eq. (2-15), and then two methods of activation energy estimation were employed as shown in Appendix B-1. Firstly, the model-fitting kinetic analysis was calculated by computer programming. The reaction rate constants (k) of each temperature were found out and then $-\ln k$ were plotted versus 1/T. The activation energy can be found from the slope of the plot. It resulted that these conversion were best fit with the first-order model as presented in Figure 4.21. The Visual Basic code of this calculating program shows in Appendix B-2.

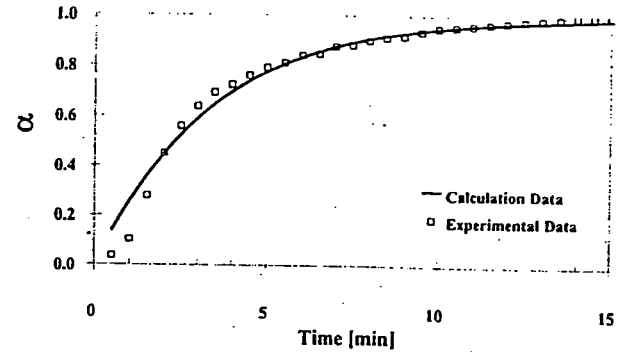

(a) EVA-33/ Dialkyl peroxide compound.

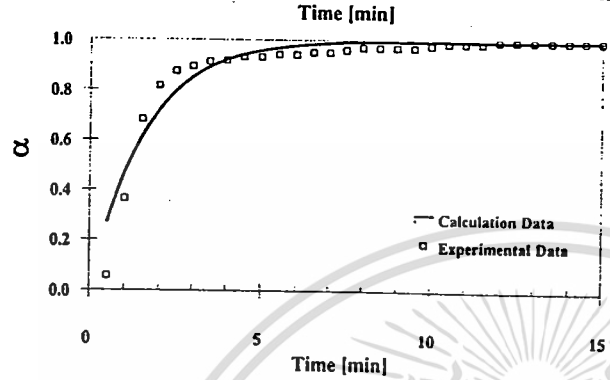

(b) EVA-33/ Peroxyester peroxide compound.

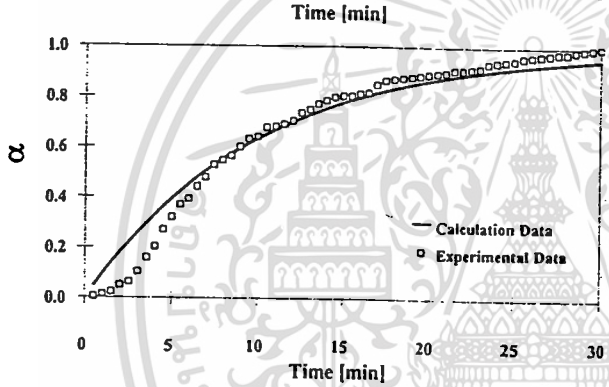

(c) EVA-33/ Peroxyketalperoxide compound.

Figure 4.21 Plots of conversion versus time of EVA-33/ Peroxides compounds at cure temperature 150°C for cure time 15 min.
(—) Calculation data (computer programming: first-order reaction).
(□) Experimental data (Eq. 2-15).

The activation energies estimated by the model-fitting method are 94, 78 and 98 kJ/mol for the EVA-33/Dialkly peroxide, EVA-33/Peroxyester peroxide and EVA-33/Peroxyketal peroxide, respectively. It can be seen that the activation energy of EVA-33/Peroxyester is lowest because the peroxyester peroxide decomposed to quite symmetric strong radicals same as the decomposition of the dialkyl peroxide but it has lower half-life temperature comparing with the dialkyl peroxide. In order to consider the complexity of free radicals generated by peroxyester and peroxyketal peroxides, the peroxyketal peroxide can produce mixture of strong and weak radicals which can initiate more complex crosslinking reactions than free radicals from the peroxyester peroxide even though these peroxide have the half-life temperature in the same range.

Due to the crosslinking reactions with organic peroxide and silane coupling agent are complex so that the exact kinetic model to describe their mechanism is quite difficult to assume. Thus, one alternative model so-called the isoconversional model-free method was determined. The model-free method is an alternative technique for activation energy examination. This method finds out the reaction time (t_α) at any given extent of conversion. The conversion curves and plots of $-\ln t_\alpha$ versus 1/T of each EVA-33/Peroxides compound are presented in Appendix B-1. The activation energy by using the model-free method so called the effective activation energy as explained previously. For EVA-33/Dialkyl peroxide and EVA-33/Peroxyester peroxide, they can be estimated approximately 96 and 75 kJ/mol, respectively as shown in Figure 4.22. They are quite similar to the activation energy from the model-fitting method. So the model-free method can be used for EVA-33/Dialkyl peroxide and EVA-33/Peroxyester peroxide crosslinking reactions. On the other hand, there is high variation of activation energy for EVA-33/Peroxyketal peroxide as displayed by black triangle symbol in Figure 4.22. It should be caused by the complexity of its crosslinking reactions from the mixture of strong and weak radicals. It can be seen that the standard isoconversional model-free method is not sufficient for estimation of the activation energy for manifold reactions likewise the crosslinking reactions of EVA-33/Peroxyketal peroxide. Therefore the other technique with satisfactory prediction such as the advanced isoconversional method (AIC) [18] should be applied to determine its activation energy for the further study.

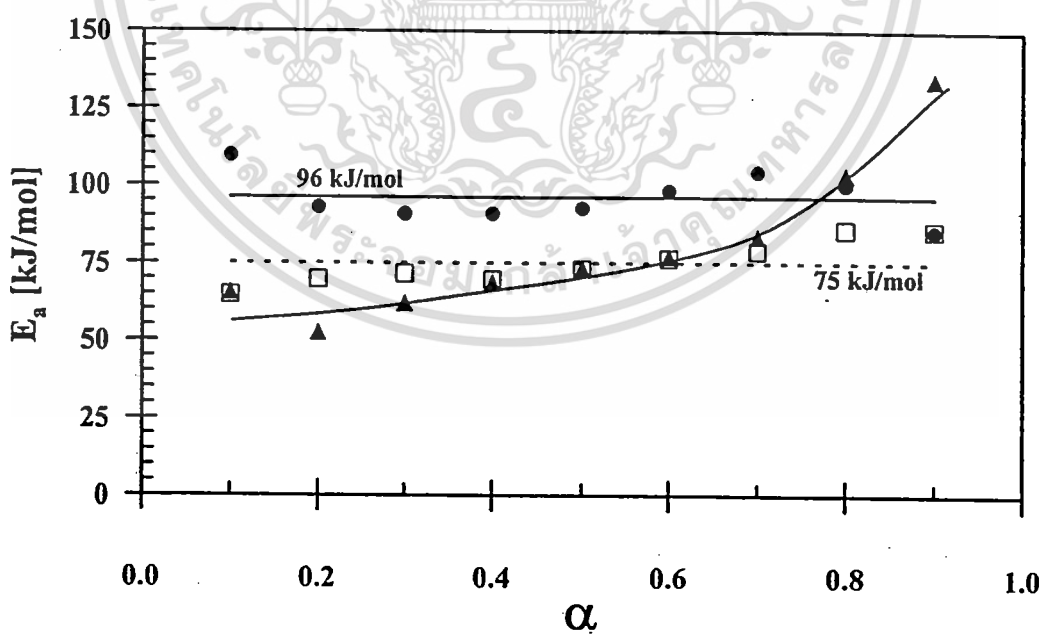

Figure 4.22 Activation energy (E_a) of crosslinked EVA-33/Peroxides compounds estimated from the isoconversional plot. (●) EVA-33/Dialkyl peroxide; (□) EVA-33/Peroxyester peroxide; (▲) EVA-33/Peroxyketal peroxide.

4.6 Gel contents of crosslinked EVA sheets

As general concept that gel content in the range of 80% or greater for cured EVA-based encapsulant is an important factor to accomplish 20-years life time service [34]. Then determination of gel content is one of investigation methods in this thesis work. The gel contents for different EVA formulations are given in Table 4.1 and 4.2. These specimens received from MDR tests. Table 4.1 shows the gel contents of EVAs/Peroxides compounds at cure temperature 150°C, 155°C and 160°C. It can be seen that all compounds at given conditions can achieve the ultimate gel content greater than 90%. Likewise the results in Table 4.2, compounds which varied peroxide concentrations can carry out high gel content greater than 90%. Since the MDR tests were operated at isothermal conditions throughout the cure test; these specimens could be cured and attained the optimum cure. So that, EVAs/Peroxides compounds which cured with perfect plateau form can produce gel content up to 80% or greater. Therefore, the encapsulant should be cured at given condition which can reach the optimum cure (i.e. plateau cure-curve) to ensure that its gel content is up to 80%. However, it is quite difficult to operate at isothermal conditions in the lamination-curing process. Thus the gel content from practical would be less than these tests.

Table 4.1 Gel contents of EVA/Peroxides compounds for cure time 15 minutes

Temperature [°C]	Gel Contents [%]			
	EVA-33/ Peroxyester	EVA-28/ Peroxyester	EVA-33/ Peroxyketal	EVA-28/ Peroxyketal
150	97.4	97.8	92.9	97.7
155	97.9	98.5	93.9	97.7
160	97.9	97.5	94.3	98.8

Table 4.2 Gel contents of EVA/Peroxides compounds for cure temperature 150°C

Peroxide Concentration [phr]	Gel Contents [%]			
	EVA-33/ Peroxyester	EVA-28/ Peroxyester	EVA-33/ Peroxyketal	EVA-28/ Peroxyketal
0.10	96.0	95.1	92.3	97.7
0.15	97.4	97.8	92.9	97.7
0.20	98.2	97.4	96.2	99.2

4.7 Light transmission of crosslinked EVA sheets

PV modules can generate electricity by converting sun light via solar cells. The incident light intensity on the PV modules affects directly to the module efficiency. Hence, the encapsulant must be transparent particularly on the front side. The light transmission for general requirement of the front-sheet encapsulant is ≥90% of incident. On the contrary, the back-sheet encapsulant does not need high transparent property.

In-house EVA encapsulants were cured at given conditions; cure temperature 150°C and cure time 15 minutes by using compression machine. The specimens were cut into rectangular shape and tested their transparency by UV-Vis spectrophotometer. The light transmittances are shown in Table 4.3.

Table 4.3 Light transmission of crosslinked EVA sheets at wavelength 550 nm

Conditions: cure temperature 150°C and cure time 15 minutes.

	EVA-33/ Peroxyester	EVA-28/ Peroxyester	EVA-33/ Peroxyketal	EVA-28/ Peroxyketal
Transmittance [%]	70.4	60.1	59.9	50.4
Thickness [mm]	0.48	0.51	0.46	0.50

The light transmittance of EVA-28 is lower than EVA-33 because VA content affects directly to its transparency. Furthermore, EVAs/Peroxyester sheets are moderately high transparent than EVAs/Peroxyketal sheets. Anyhow, the light transmittances of these compounds are less than 90% that would affect of scratches after removed molds from the specimens. Therefore, it should be use laminating on cover glass for measuring the practical transparency. The improvement of testing procedure is required. However, the thin film PV does not consider light incident on the encapsulant because it needs the encapsulant only on back side of solar cells to encapsulate solar cells to the backing support. In addition, the back-sheet encapsulant is not required the transparency, so that, the EVA-28 can be used for the back-sheet encapsulant.

4.8 Estimation of gel content by using MDR measurement

The gel content measurement by gel method (conventional method) according to ASTM D 2765-90 has to take long time for dissolving sample in organic solvent and drying under vacuum condition. The MDR method which measured torque during cure process is more convenient and useful than the gel method whereas this method does not straightforwardly yield in term of gel content. Thus the relationship between torques measured by MDR and gel content received by gel method would be determined.

Considering the torque (τ) is a function of active oxygen (A) and melt flow index (M). The relationship between torque and VA content of EVAs as shown in Figure 4.1 can be rearranged in term of torque-MFI relationship (i.e. $\tau = \tau(M)$). Likewise, the corresponding of torque and active oxygen which demonstrated in Figure 4.8 can be addressed as $\tau = \tau(A)$, so that, it can be written in form of $\tau = \tau(A, M)$ and then applying the exact differential equation to establish the relationship as follows Eq. (4-1)

$$d\tau = \left(\frac{\partial \tau}{\partial A}\right)_M dA + \left(\frac{\partial \tau}{\partial M}\right)_A dM \qquad (4\text{-}1)$$

Then define 2 coefficients: Active Oxygen coefficient (α) and Hardness coefficient (β).

Active Oxygen coefficient describes the characteristics of torque which are affected by active oxygen content or free radical initiator during the crosslinking reactions.

$$\alpha = \frac{1}{\tau_0}\left(\frac{\partial \tau}{\partial A}\right)_M \qquad (4\text{-}2)$$

Where τ_0 is the reference torque. The EVA-33, which is a commercial resin for encapsulant as well as easily melt and high MFI was chosen to be the reference resin. In order to determine the suitable reference peroxide, the lowest active peroxide, i.e. DCP, was selected. Thus, this experiment uses the maximum torque of EVA-33/DCP at given cure temperature 150°C and cure time 30 min for the reference ($\tau_0 = 1.91$ dNm).

Substituting the slope of a plot of maximum torque versus active oxygen as shown in Figure 4.23 in Eq. (4-2) gives the active oxygen coefficient. α is 0.05387 [-].

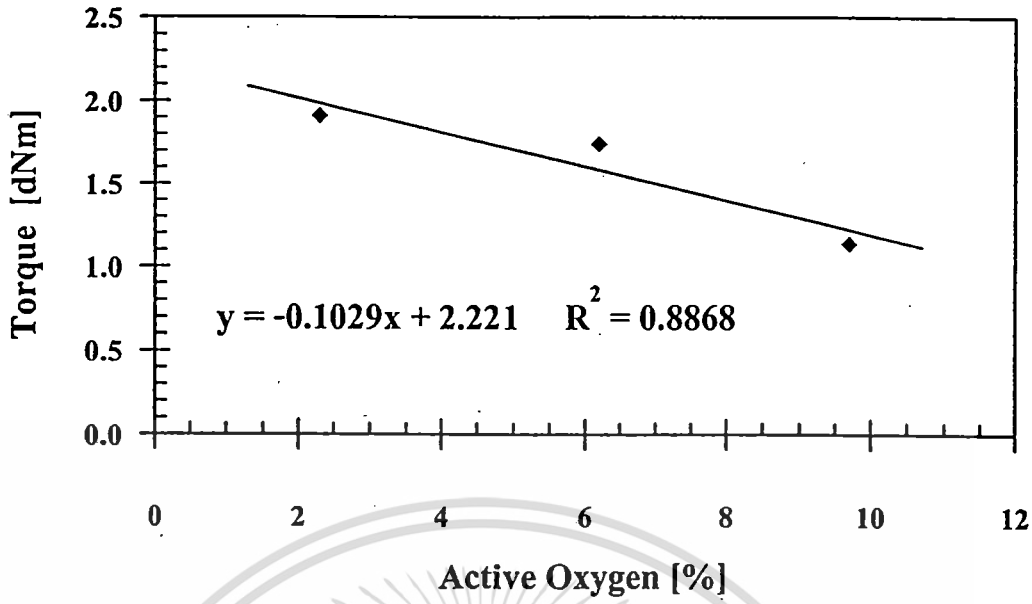

Figure 4.23 Plots of torque versus active oxygen of EVA-33/Peroxides at cure temperature 150°C for cure time 15 min.

Hardness coefficient expresses the characteristics of torque which are affected by hardness of EVA resin that caused of the melt flow index of each resin.

$$\beta = \frac{1}{\tau_0}\left(\frac{\partial \tau}{\partial M}\right)_A \tag{4-3}$$

Substituting the slope of a plot of maximum torque versus melt flow index as shown in Figure 4.24 in Eq. (4-3) gives the hardness coefficient. β is 0.00958 [g/10 min]$^{-1}$.

Substituting Eq. (4-2) and (4-3) into Eq. (4-1) and integration gives

$$\frac{\tau - \tau_0}{\tau_0} = \alpha(A - A_0) + \beta(M - M_0) \tag{4-4}$$

where A_0 is the reference active oxygen. This experiment uses the active oxygen of DCP as the reference (A_0= 2.3%). M_0 is the reference melt flow index. This experiment uses the melt flow index of EVA-33 as the reference (M_0= 30 g/10min).

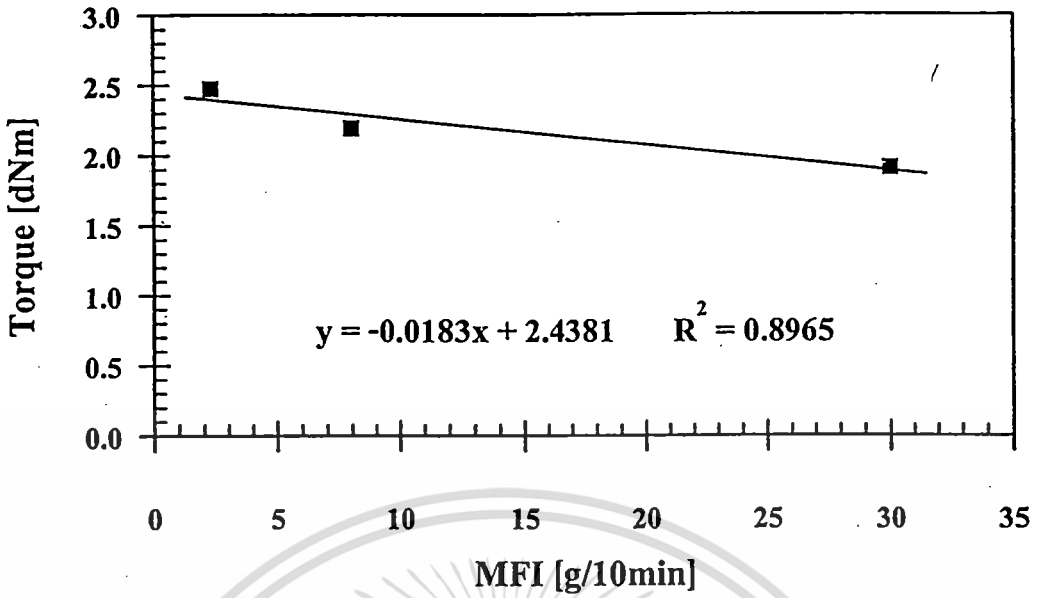

Figure 4.24 Plots of torque versus MFI of EVAs/DCP at cure temperature 150°C for cure time 15 min.

Gel contents of EVAs/Peroxides compounds at cure temperature 150°C for cure time 15 min measured by the gel method were plotted versus $(\tau-\tau_0)/\tau_0$ ratio as shown in Figure 4.25. The relationship between gel content and $(\tau-\tau_0)/\tau_0$ ratio addresses in Eq. (4-5)

$$Gel\ content\ [\%] = 4.6061\left(\frac{\tau-\tau_0}{\tau_0}\right)+96.303 \qquad (4\text{-}5)$$

Substituting $(\tau-\tau_0)/\tau_0$ ratio from MDR measurement in Eq. (4-5) then gives the gel content. Figure 4.26 demonstrates the comparison of gel content measured by Gel Method and MDR Measurement. It can be seen that the gel content by MDR measurement is similar to the gel method. The difference of two methods is less than 3%. Therefore, the estimation of gel content by MDR measurement can be provided reliable result and comfortable measurement.

This correlation would be useful applying to the encapsulant inspection in the PV industry because the gel method can not accomplish the productivity. Moreover, the gel method has to use organic solvent that is a toxic volatile material which harm to human and environment.

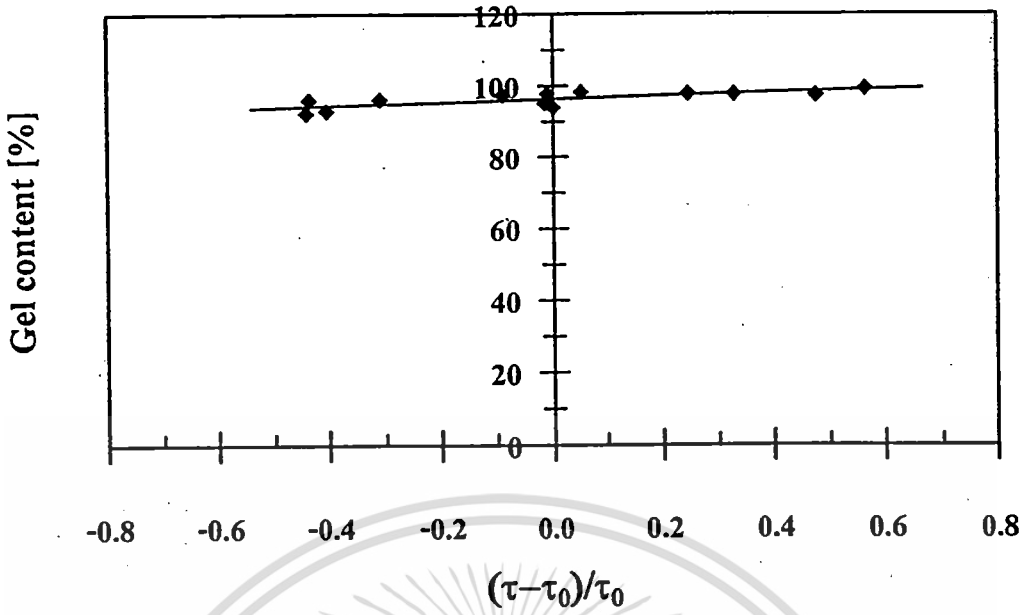

Figure 4.25 Plots of gel content versus $(\tau-\tau_0)/\tau_0$ ratio of EVAs/Peroxides at cure temperature 150°C for cure time 15 min.

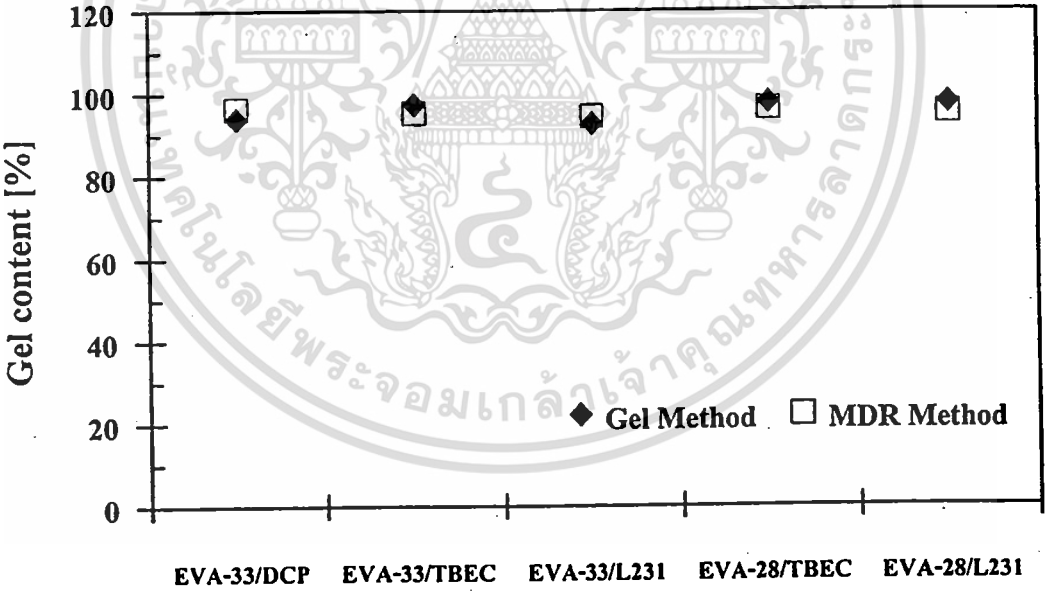

Figure 4.26 Comparison of gel content measured by Gel Method and MDR Measurement.

Chapter 5

Conclusion and Suggestions

5.1 Conclusion

The study and development of EVA-based encapsulant for solar cells contribute to the enlargement of knowledge involve the encapsulant and modification of its formula. EVAs which contain 18, 28 and 33 %wt VA contents were determined. EVA-28 is a domestic resin would be used instead of EVA-33 (imported-commercial EVA grade) because its physical property and crosslinking characteristics are proper to the encapsulation material.

The important key factor of crosslinking reactions of EVA-based encapsulant during lamination-curing process is organic peroxide. Three classes of organic peroxide candidates which are (1) dialkyl peroxide; (2) peroxyester peroxide; and (3) peroxyketal peroxide were studied. Dialkyl peroxide is not suitable because it has high half-life temperature and its by-products can discolor the final product. Peroxyester peroxide as a commercial is good for curing at temperature in range of 150 to 160°C which accomplished ultimate cure within 5 to 8 minutes. Moreover, peroxyketal peroxide has higher performance which decreased optimum cure time to 3 minutes. Furthermore, the EVA-28 compounded with 0.10 phr of peroxyketal peroxide has considerably good performance for the encapsulant formulation.

The gel contents of in-house formulations are up to 90% but the light transmittances are moderately low due to their surface damage from mold removing. Although light transparency does not attain for the front-side encapsulant requirement, it can be used for the back-side encapsulant for crystalline solar cells and thin film solar cells which use only back-side encapsulant. Thus, it would be possible to use the domestic EVA for PV encapsulant

This research applied the MDR to determine crosslinking behavior. This apparatus is suitable for real-time isothermal crosslinking reaction study. Isothermal isoconversional model-free method was employed for kinetic analysis. The effective activation energy as a parameter measured from a temperature dependence of the overall reaction rate was calculated and compared to the results from the model-fitting method by using computer programming. The activation energies estimated by the model-fitting method are 94, 78 and 98 kJ/mol for the EVA-33/Dialkly peroxide, EVA-33/Peroxyester peroxide and EVA-33/Peroxyketal peroxide, respectively. In addition the activation energy by using the model-free method of

EVA-33/Dialkyl peroxide and EVA-33/Peroxyester peroxide can be estimated approximately 96 and 75 kJ/mol but it is not sufficient for estimation of the activation energy for manifold reactions likewise the crosslinking reactions of EVA-33/Peroxyketal peroxide.

Furthermore, the MDR measurement can be used to estimate the gel content by using the correlation of torque ratio $(\tau-\tau_0)/\tau_0$ which achieved the difference less than 3% from the conventional gel method.

5.2 Suggestions

This research should be adjusted in some points as follows:

1. The other properties such as mechanical properties and weatherability should be test.

2. The blend effect of the domestic and commercial EVA resin is interesting to study because it can reduce the total cost.

3. The sample preparation for light transmittance test should be modified and lamination by using the vacuum laminator should be applied to the test.

References

[1] Boyle G. **Renewable Energy: Power for a Sustainable Future.** 2nd ed., Oxford University Press, UK, 2004.

[2] European Commission, DG Joint Research Centre, **PV Status Report 2006, Research, Solar Cell Production and Market Implementation of Photovoltaics.** Institute for Environment and Sustainability, Renewable Energies Unit, Italy, August 2006.

[3] Sterzinger G., M. Svrcek. **Solar PV Development: Location of Economic Activity.** Renewable Energy Policy Project,Technical Report, January 2005.

[4] Czanderna A.W., Pern F.J. "Encapsulation of PV modules using ethylene vinyl acetate copolymer as a pottant: A Critical review." **Solar Energy Materials and Solar Cells** . vol.43. 1996 pp. 101-181.

[5] Klemchuk P., Ezrin M., Lavigne G., Holley W., Galica J., Agro S. "Investigation of the degradation and stabilization of EVA-based encapsulant in field-aged solar energy modules." **Polymer Degradation and Stability.** vol. 55, 1997. pp. 347-365.

[6] Specialchem4polymer, "Ethylene copolymers" [Online]. Available: http://www.specialchem4adhesives.com/tc/ethylene-copolymers. 2005.

[7] Harper C.A., Petrie E.M. **Plastics Materials and Processes, A Concise Encyclopedia.** Wiley-interscience, New York, USA, 2003.

[8] Product Bulletin, Organic peroxides: General Catalog. Arkema Inc., USA. 2006.

[9] Dick J.S. **Rubber Technology: Compounding and Testing for Performance.** Hanser Publishers, Munich, 2003.

[10] Specialchem4polymer, "Organic Peroxides Crosslinking Agents" [Online]. Available: http://www.specialchem4polymers.com/tc/Organic-Peroxides-Crosslinking-Agents. 2005.

[11] A Guide to Silane Solutions from Dow Corning, Dow Corning Corporation, USA, 2005.

[12] Fogler H.S. **Elements of Chemical Reaction Engineering.** 3rd ed., Prentice Hall PTR, New Jersey, USA, 1999.

[13] Thaworn T., Sermdararat S, Lohsiwanont W., Areerat S., Namkanisorn A. "Study of crosslinking mechanism of ethylene vinyl acetate (EVA) encapsulating materials for solar cell," **Proceedings of the 14th Thai Chemical Engineering and Applied Chemistry.** Bangkok, Thailand, 2004, pp. A7:1-11. (in Thai).

[14] Mishra S., Baweja B., Chandrd R., "Studies on Dynamic and Static Crosslinking of Ethylene Vinyl Acetate and Ethylene Propylene Diene Tercopolymer Blends." **Journal of Applied Polymer Science.** vol. 74, 1999. pp. 2756-2763.

[15] Parent J.S., Geramita K., Ranganathan S., Whitney R.A. "Silane-Modified Poly(ethylene-co-acetate): Influence of Comonomers on Peroxide-Initiated Vinylsilane Grafting." **Journal of Applied Polymer Science.** vol. 76, 2000. pp. 1308-1314.

[16] Bounor-Legaré V., Ferreiea I., Verbois A., Cassagnau P., Michel A. "New Transesterification between Ester and Alkoxysilane Groups: Application to Ethylene-co-Acetate Copolymer Crosslinking." **Polymer.** vol.43, 2002. pp. 6085-6092.

[17] Hunt B.J., James M. I. **Polymer Characterisation.** Blackie Academic & Professional, London, 1993.

[18] ASTM D 5289-97, "Standard Test Method for Rubber Property-Vulcanization Using Rotorless Cure Meters." **Annual Book of ASTM Stands,** vol. 09.01, 1995.

[19] Dick J.S. **Basis Rubber Testing: Selecting Methods for a Rubber Test Program.** ASTM Stock Number: MNL39, USA, 2003.

[20] Dick J.S., Pawlowski H. "Applications for the Curemeter Maximum Cure Rate in Rubber Compound Development Process Control and Cure Kinetic Studies", *Polymer* **Testing.** vol. 15, 1996. pp. 207-243.

[21] Khawam A., Flanagan D.R. "Role of Isoconversional methods in varying activation energies of Solid-State Kinetics I: Isothermal Kinetic Studies." **Thermochimica Acta.** vol. 429, 2005. pp. 93-102.

[22] Sbirrazzuoli N., Mititelu-Mija A., Vincent L., Alzina C. "Isoconversional Kinetic Analysis of Stoichiometric and Off-Stoichiometric Epoxy-Amine Cures." **Thermochimica Acta.** vol. 447, 2006. pp. 167-177.

[23] Salla J.M., Ramis X., Morancho J.M., Cadenato A. "Isoconversional Kinetic Analysis of a Carboxyl Terminated Polyester Resin Crosslinked with Triglycidyl Isocyanurate (TGIC) used in Power coatings from Experimental Results Obtained by DSC and TMDSC." **Thermochimica Acta**. vol. 388, 2002. pp. 355-370.

[24] ASTM D 2765-90, "Standard Test Method for Determination of Gel Content and Swell Ratio of Crosslinked Ethylene Plastics." **ASTM Annual Book of ASTM Standard**. vol. 09.01, 1998.

[25] SOLAR EVA®, Technical Information, Hi-Sheet Industries, Ltd., Japan. 2004.

[26] U.S. Department of Energy; Energy Efficiency and Renewable Energy, "Solar Energy Technologies Program: Light and the PV Cell" [Online]. Available: http://www1.eere.energy.gov/solar/pv_cell_light.html

[27] Light Transmission and Reflectance, Technical Data, CYRO Industries, NJ, USA, 2001.

[28] Pavia D.L, Lampman G.M., Kris G.S. **Introduction to Spectroscopy: A Guide for Student of Organic Chemistry**. 3rd ed., Thomson Learning, Washington, USA, 2001.

[29] Cuddihy E.F., Coulbert C.D., Willis P., Baum B., Garcia A., Minning C. "Polymeric Encapsulation Materials for Low-Cost, Terrestrial, Photovoltaic Modules." **Polymers in Solar Energy Utilization, ASC Symposium Series 220**, American Chemical Society, Washington, 1983. pp. 353-366.

[30] Lewis K.J. "Encapsulant Material Requirements for Photovoltaic Modules." **Polymers in Solar Energy Utilization, ASC Symposium Series 220**, American Chemical Society, Washington, 1983. pp. 367-385.

[31] Burger D.R., Cuddihy E.F. "Vacuum Lamination of Photovoltaic Modules." **Polymers in Solar Energy Utilization, ASC Symposium Series 220**, American Chemical Society, Washington D.C., 1983. pp. 407-419.

[32] Pern F.J. "Factor That Affect the EVA Encapsulant Discoloration Rate upon Accelerated Exposure." **Proceeding of IEEE First World Conference on Photovoltaic Energy Conversion**, Hawaii, USA, December 5-9, 1994. pp. 897-900.

[33] Galica J.P., Sherman N. "Results to Date-Development of New EVA-Based Encapsulants, Faster-Curing and Flame-Retardant Types." **Proceeding of Photovoltaic Specialists Conference**, Anchorage, AK, USA, September 15-22, 2000. pp. 30-35.

[34] Wohlgemuth J., Shea S. **PVMat Improvements in the BP Solar Photovoltaic Module Manufacturing Technology**. Final Subcontract Report, NREL/SR-520-32066, Maryland, April, 2002.

[35] Agro S.C., Tucker R.T. **Development of New Low-Cost, High-Performance, PV Module Encapsulant/Packing Materials**. Annual Technical Report, Phase 1, NREL/SR-520-35683, Connecticut, March, 2004.

[36] Evaflex® Grades, Technical Data Sheet, DuPont-Mitsui Polychemicals Co., Ltd., Japan. 2005.

[37] Ethylene Vinyl-Acetate Polene MV 1055, Technical Data Sheet, IRPC, Thailand. 2006.

[38] Pern F.J., Glick S.H. "Thermal Processing of EVA Encapsulants and Effects of Formulation Additives." **Proceeding of Photovoltaic Specialists Conference**, Washington D.C., USA, May 13-17, 1996. pp. 1251-1254.

[39] Vyazokin S. "Reply to "What Is Meant by the Term 'Variable Activation Energy' When Applied in the Kinetics Analyses of Solid State Decompositions (Crystolysis Reactions)?"." **Thermochimica Acta**, vol. 397, 2003. pp. 269-271.

[40] Sbirrazzuoli N., Vyazovkin S. "Learning About Epoxy Cure Mechanisms from Isoconversional Analysis of DSC Data." **Thermochimica Acta**, vol. 388, 2002. pp. 289-298.

[41] Vyazovkin S., Wight C.A. "Model-Free and Model-Fitting Approaches to Kinetic Analysis of Isothermal and Nonisothermal Data." **Thermochimica Acta**, vol. 340-341, 1999. pp. 53-68.